Highly Miniaturized Robots for Inspection of Small Nuclear Piping

Nikhil Jog

CMU-RI-TR-19-13
May 2019

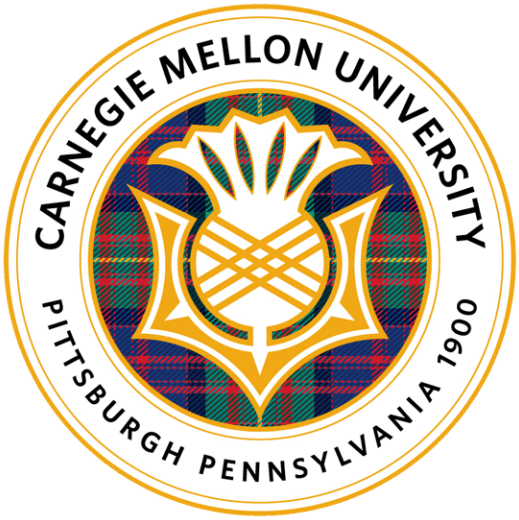

The Robotics Institute
School of Computer Science
Carnegie Mellon University
Pittsburgh, PA 15213

Thesis Committee:
William "Red" Whittaker, Chair
John M. Dolan
Joseph Bartels

Submitted in partial fulfillment of the requirements for the degree of Master of Science in Robotics.

Abstract

Bomb-making in the 20th century resulted in the creation of massive facilities to produce Uranium. These are now defunct, heavily contaminated and facing decommissioning. As part of a multi-billion-dollar agenda, the measurement of radioactivity is required for the safe disposal of residual Uranium in piping. Existing methods involve manual cutting of asbestos-lined thermal enclosures and performing repeated hazardous and inaccurate measurements of radiation from the outside. Manual techniques have proven too approximate, slow and inefficient for this need. Robots, as addressed here, perform accurate, efficient measurement by operating from the inside and viewing the Uranium directly on the interior of the pipe walls.

Carnegie Mellon University has already developed a first-of-kind robot, RadPiper, to address this problem within the largest of these pipes. Development of the large robot had the advantage of big mobility, big batteries, big computing, big sensors and a big radiation detector. The compelling need is the development of a family of such robots for service in the full range of smaller sizes important in these facilities.

This paper describes the development and technical details of a modular robot, NanoPiper, to operate inside the smallest, 3", piping within these facilities. NanoPiper development has the challenge of constraint to miniaturized mobility, small batteries, small computing, small sensors and a small radiation detector. This miniaturization is so profound that there is a fundamental question of possibility, and success is not foregone. The principles, configuration, and manifestation of such a device are the distinctions of this research.

NanoPiper builds a robust and accurate radioactive model using newly invented acoustic localization, state-of-the-art geometric profiling and miniaturized radiation sensing. Its autonomous robotic in-pipe functionality delivers the precision, repeatability, and certainty unachievable by traditional manual methods.

Creation of NanoPiper is the case proof that the robot for the smallest relevant pipe size is achievable. This exhibits that a family of robot sizes is feasible for all intermediate pipe sizes from those serviced by RadPiper down to those serviced by NanoPiper. The technology is a transformational contribution to the nuclear cleanup industry.

Acknowledgements

I would like to thank my advisor, Red Whittaker, for giving me the opportunity to perform research all those years ago. I started out as an engineer who didn't know what to do outside of schoolwork. Despite my limited experience, he wholeheartedly took me on and gave me a chance to work on projects that had a direct ability to save lives and advance scientific progress. Under his guidance and involvement, I learned how to approach scientific problems and build systems that help people. Thank you to my committee members, John Dolan and Joe Bartels, for their feedback and design advice throughout the project.

Thank you to Chuck Whittaker and Tim Angert for taking an electrical and software guy and turning him into a "somewhat decent machinist." Without them, this project would have been a mechanical impossibility.

Thank you to my fellow lab members, Andrew Zhang, David Kohanbash, Eagle Zhao, Heather Jones, Jim Teza, Jordan Ford, Josh Spisak, Ralph Boirum, and Siri Maley for helping me figure out everything that had to go into NanoPiper. From the radiometry to robot design to robot software and testing, each one of them helped make NanoPiper possible.

Thank you to the DE-EM0004067 DOE Traineeship in Robotics at Carnegie Mellon University for funding this research.

This page is intentionally left blank.

Contents

This page is intentionally left blank.

List of Figures

List of Tables

Introduction

Bomb-making in the 20th century resulted in the creation of massive facilities to produce Uranium. These are now defunct, heavily contaminated, and facing decommissioning. Vast amounts of Uranium-235 (U-235) remain in miles of piping that once enriched America's Uranium.

Figure 1: Leftover deposit in 42" piping (left). Manual inspection of small piping (right).

The immense schedule and budget driver is the requirement to determine the exact number of grams of U-235 per foot of pipe before demolition. Pipes containing less U-235 than the 'criticality incredible' threshold are candidates to leave and demolish in place, but pipes containing unsafe amounts of fissile material require costly removal and management before disposal.

To date, human workers in protective clothing have manually deployed detectors from outside of these pipes to observe the radiation emitted from the deposit inside (Figure 1) [1] [2]. This incurs the operational disadvantages of clearing around pipes for access, hazards of elevated work, radiation exposure and manual data transcription. The technical disadvantages include faint signal from attenuation through pipe walls, inability to directly view deposits, and inability to position a detector at the center of the pipe.

The real crux of measurement operations is the transcription of data, analysis, reporting, review and archiving that follows the data gathering [3]. Data are transcribed manually, analyzed by humans and then reported in documents that are also manually generated. This method is subject to errors, misinterpretations, costs, and long delays.

Motivation

Manual inspection methods have proven too slow, ineffective, inaccurate and costly to collect and analyze. Robotic inspection provides compelling advantages derived from in-pipe measurement:

1. Requires little-to-no modification of existing infrastructure for access
2. Precludes significant elevated and dangerous work for NDA personnel
3. Achieves superior speed, accuracy and certainty versus external, through-wall methods
4. Provides automatic data collection, screening, reporting and archiving
5. Captures radiometric, geometric and visual record of deposit
6. Generates redundant measurements for validation
7. Achieves vast schedule and budget economy for decontamination and decommissioning of Uranium enrichment sites

Automated analysis and reporting tools greatly reduce manual intervention and provide a more consistent examination [3]. Manual methods require up to five man-hours per foot of inspection, while autonomous methods can inspect and analyze entire 100-ft. pipe segments in less than two hours.

As autonomous inspection robots mature, it will be possible to autonomously inspect piping of all sizes at a fraction of the cost and time.

Prior Work

The Pipe Crawling Activity Measurement System (PCAMS) developed by Carnegie Mellon University is a pioneering system for robotic non-destructive assay (NDA) of radioactive pipes. Prior work focused on the creation of a single class of robots for the 30" and 42" pipe sizes. This robot, known as RadPiper, was the initial foray to develop a radiation model of the Uranium-235 (U-235) inside the pipes of the DOE Portsmouth Gaseous Diffusion Enrichment facility.

RadPiper was the first autonomous robotic crawler for NDA [4]. It removed the requirement for manual measurements of decommissioned pipes. This pipeline has been extensively tested by DOE technicians and analysts and is currently undergoing commissioning on-site [3].

The following discussions of RadPiper's sensing, localization, and more broadly of pipe robots provide more specific context based on which miniaturized Uranium measuring robots are investigated in this research.

1.1. Sensing

RadPiper uses a sodium iodide scintillation detector in a unique disc-collimated assembly capable of segmenting the pipe wall. This internal measurement greatly increases the incoming count rate of the U-235, which results in a more accurate radiation model. However, its large detector size limits its applicability within smaller pipes. There needs to exist a sensor capable of measurement in pipes as small as 3". Small detectors are the result of major breakthroughs in instrument-grade spectrometers. Newly invented detectors are on the scale of a single inch, making them amenable to integration within small pipe sizes.

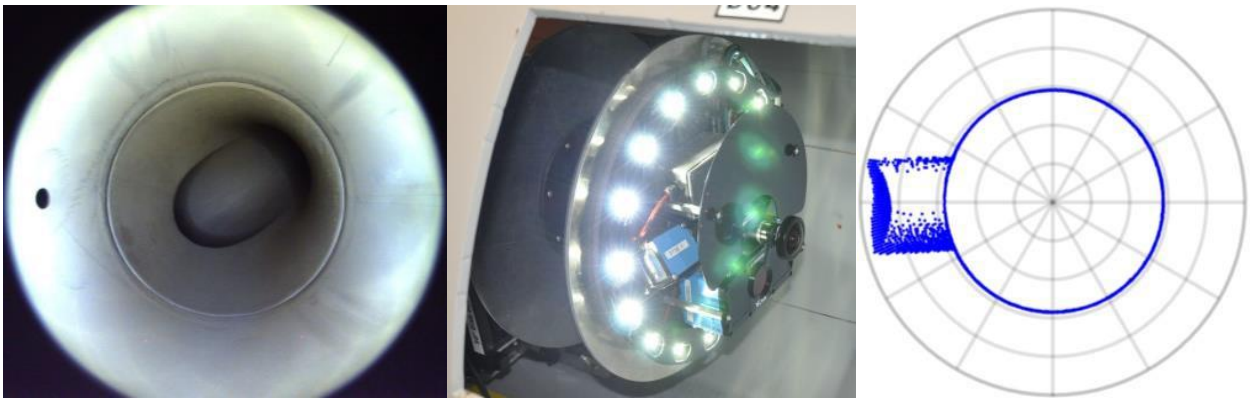

Figure 2:In-pipe imagery (left). Sensor payload (center). Geometric modelling results (right).

RadPiper uses numerous auxiliary sensors in addition to the radiation sensor to provide radiation estimates. RadPiper features a large, vision-grade fisheye camera in conjunction with a rotational LIDAR scanner to provide analysts with additional information to validate radiometric predictions or to flag for further manual inspection (Figure 2). The large sizes of this camera and LIDAR scanner are intractable for a miniaturized rover. Other superb miniaturized cameras and lenses are available as components for smaller robots.

Existing technology for LIDAR focuses on mapping of large objects at medium-to-long distances. With minimum sensing ranges of three inches, these systems are incapable of taking measurements within three-inch or six-inch pipes. Further innovation is required to develop a scalable sensor capable of measurements at the smaller pipe sizes.

1.2. Localization

The crux of any robotic pipe inspector is to quantify observables and correlate them with a location within a pipe. The capability is denoted as 'localization'. Localization for gas and sewage pipes uses encoded tethers or visual odometry. Encoded tethers are a complexity and hazard to nuclear operations where contamination and transport of isotopes are forbidden. These pipes also demonstrate easily identifiable features, such as valves or exposed brick, neither of which are present in nuclear piping.

Figure 3: Tethered pipe inspection robot (left). Inside of nuclear piping displaying a distinct lack of features (right).

RadPiper localization, which is the only precedent in nuclear piping, is primarily done through a pair of low-resolution encoders in conjunction with a high-resolution laser range finder. This class of high-resolution, survey-grade range finders is far too large for deployment on the small robots conceived in this research. For long pipe runs, in-pipe artifacts and robot pose preclude continuous registration against the starting launch rig. Experimental results have shown consistent readings from this range finder up to 50 feet with intermittent readings up to 100 feet. Fusion of the various sensor data in post-processing greatly reduces the uncertainty of robot state estimation. Nevertheless, such a system is susceptible to drift in long-range operation. With high-precision laser measurement absent at long ranges, RadPiper effectively has a maximum inspection distance of 100 feet.

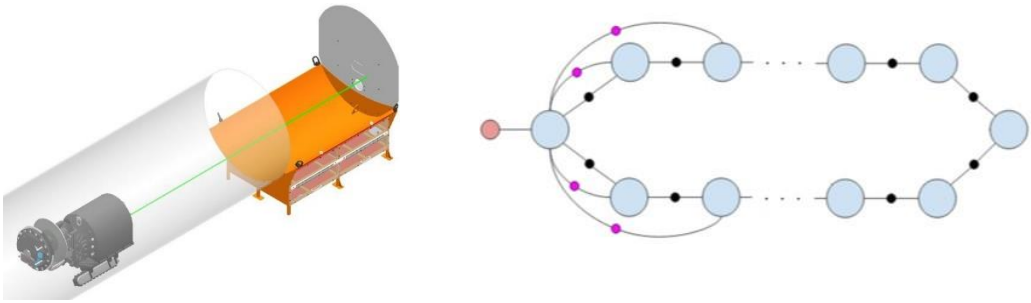

Figure 4: Factor graph optimization fuses high-accuracy laser measurements (pink) with low-accuracy encoder data (black) to perform better state estimation.

PCAMS uses factor graph optimization (Figure 4), a state-of-the-art method for solving simultaneous localization and mapping (SLAM) problems, to probabilistically localize the robot along the forward and reverse pipe length. Experimental results have shown maximum drifts of 10-20 mm over repeated 30m runs (Figure 5) using the sensor package on RadPiper, setting a baseline for localization for nuclear robots.

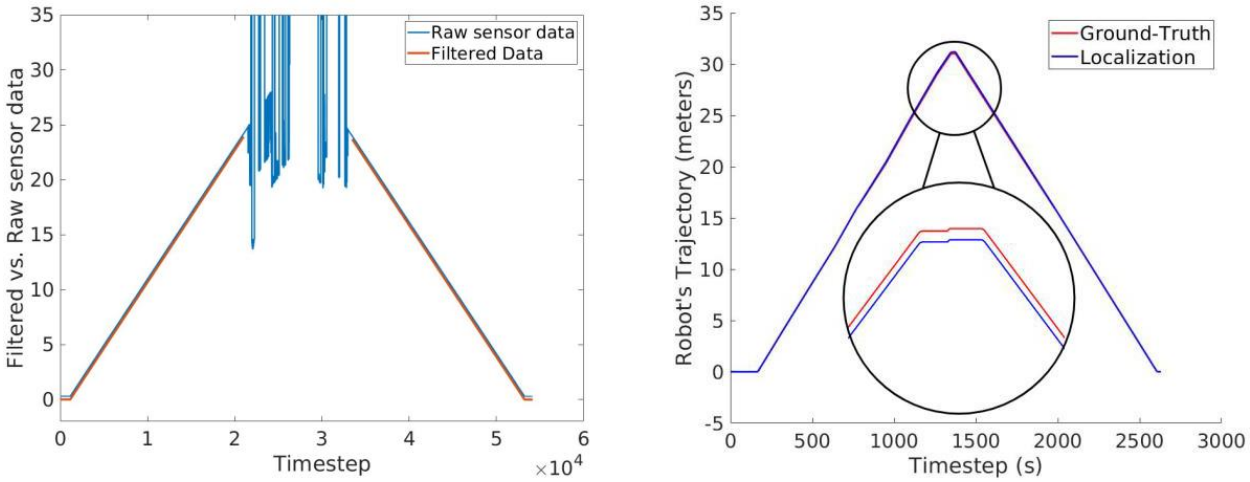

Figure 5: Raw odometry measurements (left). Corrected odometry results (right).

PCAMS RadPiper has validated the most difficult radiometric challenge in 30" and 42" piping while providing numerous augmentations onto manual inspection methods. PCAMS NanoPiper seeks to build upon this success by pioneering a solution for the most difficult mechatronics challenges within 3" piping.

1.3. Existing Pipe Robots

Pipe inspection robots have existed for decades, though none exhibit the capabilities essential for Uranium measurement. Numerous products exist in the market for inspection of pipes as small as 2 inches. Products from market-leading companies such as Inuktun and Versatrax boast industrial-quality inspection robots that are ready for delivery (Figure 6).

Figure 6: 4" pipe inspection robot from Inuktun (left). 2" pipe inspection robot from HoneyBee (right).

Unique features such as magnetic wheels [5] and low-profile treads [6] enable them to carry larger payloads and inspect varying pipe geometries. However, they are severely lacking in both ease of operation and versatility. These products were designed for manual inspections of particular pipe sizes and do not carry the sensor suite required for universal usage.

All products on the market are tethered and manually operated, making them non-viable for radiometric inspections due to a lack of precisely controlled speed, centering, and steering unachievable by teleoperation. The robots are also single-featured, offering a simple camera with no ability to upgrade capabilities. The lack of safeguarding sensors makes autonomy for uncontrolled environments a near impossibility.

This research conceives NanoPiper as a highly miniaturized robot for inspection of small nuclear piping. It seeks to provide the only radiometric solution for small piping by addressing the needs for autonomy, tetherless operation, precise localization, and geometric and radiometric mapping while also providing customizable solutions for varied use cases.

PCAMS Family of Robots

PCAMS aims to develop mechatronic models for five distinct size classes:

1. RadPiper (42” / 30”)
2. RadPiper Jr. (36” / 24”)
3. MiniPiper (20” / 16” / 14”)
4. MicroPiper (12” / 10” / 8”)
5. NanoPiper (6” / 4” / 3”)

This thesis aims to characterize the mechatronic scaling characteristics governing the smallest class of robots in such a manner that intermediate robots can be designed by scaling up or down individual components. As a result, RadPiper Jr. and MicroPiper will be very similar to RadPiper and NanoPiper, respectively.

Figure 7: RadPiper (top-left). Concept designs for RadPiper Jr. (top-center), MiniPiper (top-right), MicroPiper (bottom-left) and NanoPiper (bottom-right).

Every pipe robot is fundamentally a platform to carry a radiation detector at the center of the pipe. The geometric constraints of such an undertaking are the primary cause of the breakpoints between each class of robot sizes. Bigger pipe sizes require larger radiometric assemblies that are often the heaviest parts of the system. Centering a detector within a larger pipe requires taller assemblies which shifts the center of mass. At a certain pipe size, these assemblies become disproportionately larger than the base, leading to an unstable robot. The above size cutoffs minimize the number of robots required while maximizing robot capabilities.

2.1. Functional Requirements

NanoPiper's fundamentally has a few requirements regarding size, weight, and flexibility. Small batteries, small motors, small computers and small sensors preclude the use of large, heavy robots. Furthermore, NanoPiper must operate without any infrastructure modifications, thereby eliminating the use of established methodologies such as GPS or building sensors. A key differentiator of NanoPiper is its flexibility; the same base design must be usable for multiple pipe sizes and scenarios with little-to-no modification. Ultimately, the most difficult challenge is to fit inside a 3" pipe.

Table 1: Functional requirements for NanoPiper

Configuration	Localization	Mapping	Navigation	Autonomy	Mobility
1.1) < 10 kg < 36" length < 3" diameter	2.1) No artificial infrastructure (e.g. GPS, launch rig sensors)	3.1) Geometric modeling with high fidelity and resolution	4.1) 2 ft/min continuous operation	5.1) Identify positive and negative obstacles	6.1) Ascend 10-15-degree slopes and surmount 3-5 cm gaps
1.2) Easily upgradeable parts	2.2) Pipe-independent odometry with <1% error	3.2) RGB imagery of pipe interior	4.2) Operation within straight and askew pipes	5.2) Fixed or open distance operation	6.2) Active or passive centering within the pipe

2.2. Radiometric Scaling

Collimator Design

Disc-collimation is the fundamental idea on which in-pipe robotic measurement of Uranium is founded. Disc-collimation brackets a spectrometry detector with a pair of axisymmetric collimating discs that are made of shielding material such as lead. Since the isotope of interest is Uranium-235, its peak energy is only 186 keV [7], and hence a mere 0.125" of lead thickness attenuates over 99% of the relevant intensity. These discs present a cylindrical field-of-view between the detector and a segment of pipe wall.

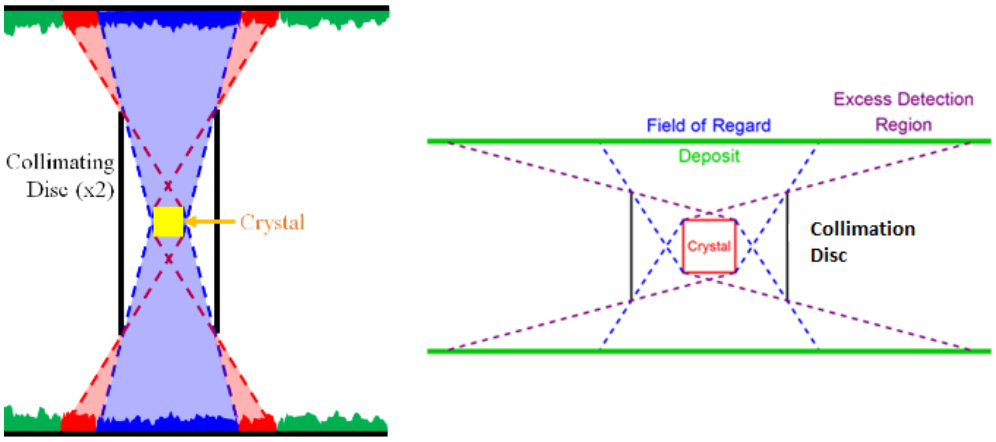

Figure 8: Crystal FOV geometries in 42" pipes (left) and 3" pipes (right).

Simultaneously, the discs preclude field-of-view from the pipe wall upstream or downstream of the detector (Figure 8). By this means, disc-collimation views only a given segment of pipe at a given time.

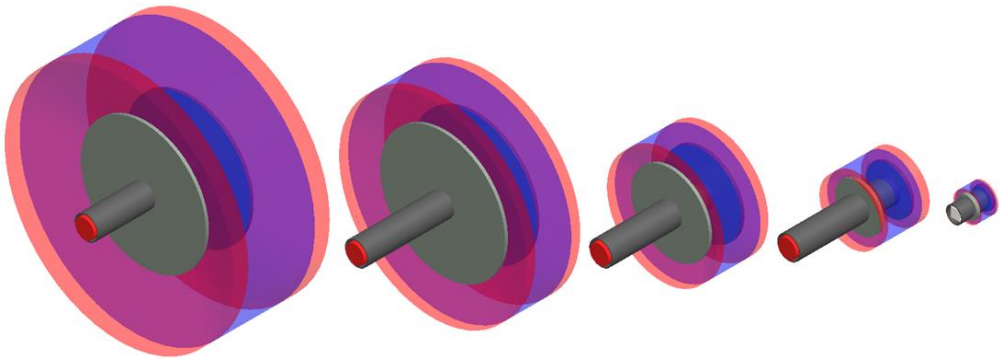

Figure 9: Disc-collimated FOV for varying pipe sizes.

Each PCAMS collimator features a distinct design balancing collimator weight, detector count rate, resolution, accuracy and clearance (Figure 9). Larger pipe sizes require larger discs to reduce the FOV of the excess detection region (Table 2). Smaller crystals reduce the count rates from radioactive materials and take up less space within the collimation. This leads to smaller collimation regions, thereby reducing the count rate further but increasing the resolution.

Table 2: Expected collimator physical characteristics in various pipe sizes.

60 lb. – ø18”	60 lb. – ø15”	20 lb. – ø10”	7 lb. – ø5”	1 lb. – ø2”
ø42” Pipes 11” FOV	ø36” Pipes 6” FOV	ø20” Pipes 6” FOV	ø12” Pipes 5” FOV	ø6” Pipes 3” FOV
ø30” Pipes 8.5” FOV	ø24” Pipes 5” FOV	ø16” Pipes 5” FOV	ø10” Pipes 4” FOV	ø4” Pipes 2” FOV
		ø14” Pipes 4” FOV	ø08” Pipes 3” FOV	ø3” Pipes 1” FOV

The mechatronic scaling of the collimator must be large enough to exclude counts outside the FOV, spaced out enough to cover the entirety of the crystal, but light enough such that it can be easily carried by the robot.

Near-field Radiation Measurements

Radiometric measurement models are heavily influenced by their distance to the source. When measuring radiation at a great distance, the source and detector can be treated as a point source which follows the inverse square law in terms of radioactive strength. This assumption holds for the largest size class but breaks down in the smallest size class. Displacements at this smaller distance produce a more linear scaling factor. Per empirical results (Figure 10), a hundredth-of-an-inch displacement produces an approximately 1% reduction in measured strength.

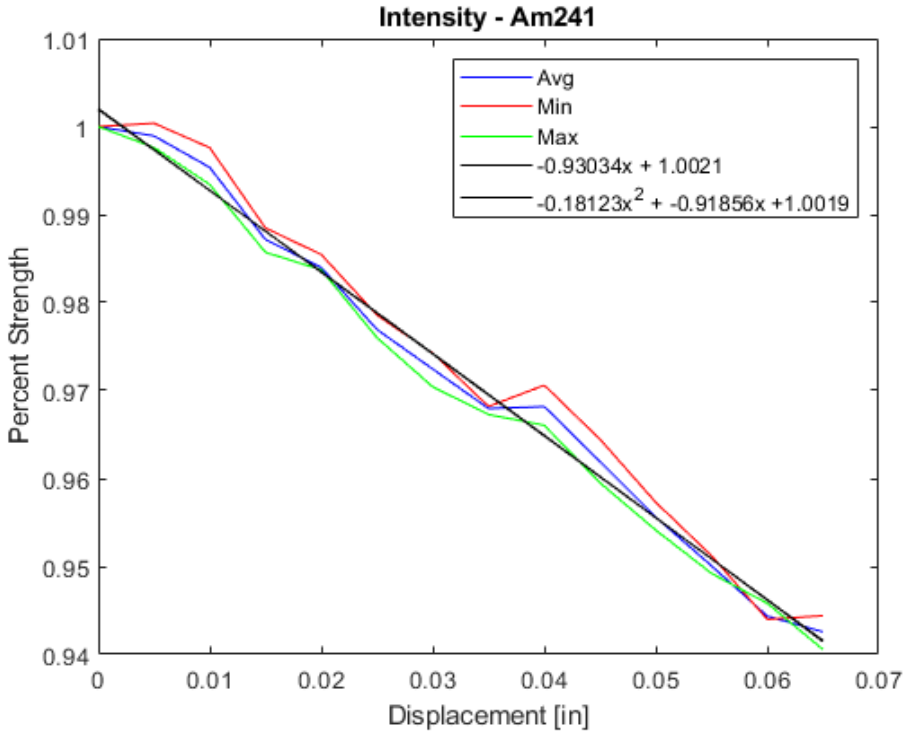

Figure 10: Normalized intensity measurements in near-field experimentation.

PCAMS RadPiper uses a scintillation detector with a cylindrical crystal of 2" (5.08 cm) in diameter and 2" (5.08 cm) in height, while PCAMS NanoPiper uses a square crystal of 0.39" (1 cm) side-length. This is a crystal volume ratio of approximately 400:1 cm^3. This reduction in volume greatly reduces the count rate of radiation events. This leads to the requirement of slower inspection speeds so that the robot can collect a statistically significant sample (Figure 11).

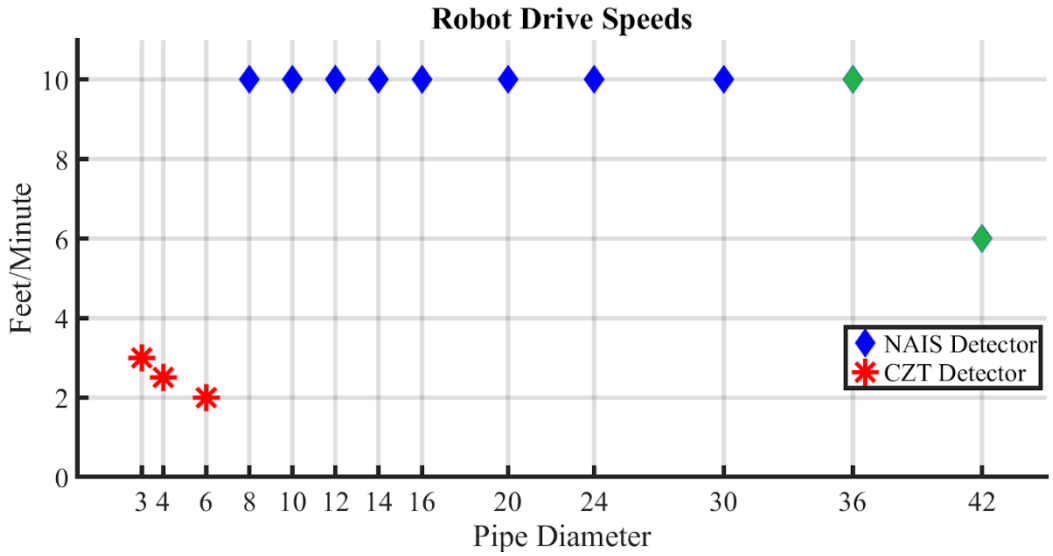

Figure 11: Reduced crystal volumes requires reduced driving speeds to allow collection of a statistically significant radiometric sample.

One solution to increase the drive speed is to place multiple detectors side-by-side to enable better accumulation of radiation events, e.g. a four-fold higher count rate enables a four-fold higher driving speed (Figure 12). Detectors are also placed closer to the radioactive material, additionally increasing the incoming count rate.

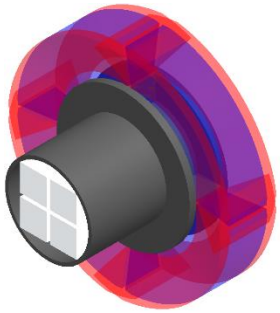

Figure 12: "Cruciform" collimation that allows a 4x increase in count rate.

Crystal Geometry and Near-field Uncertainty

When placed into a pipe, the cylindrical crystal provides an axisymmetric view of the pipe walls, while a square crystal does not. As a result, the surrounding geometry of disc-collimation differs depending on the size and shape of the crystal.

$$l = 1\ cm;\ D = 53.34\ cm$$

$$\frac{I_1}{I_2} = \frac{(D_2)^2}{(D_1)^2} = \frac{53.34^2}{\sqrt{(53.34^2 + 0.5^2)}^{\,2}} = 0.9999$$

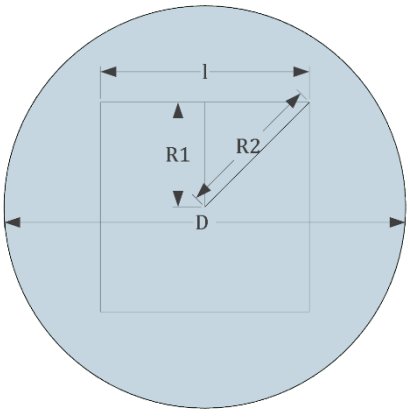

At large wall distances, this slight asymmetry does not have a noticeable effect with an intensity difference of less than 0.01%.

$$l = 1\ cm;\ D = 3.81\ cm$$
$$\Delta D = \sqrt{3.81^2 + 0.5^2} - 3.81 = 0.03266\ cm = 0.0128\ in$$

Based on the small-scale experiments this research performed on a point source, a displacement of 0.0128" produces a reduction of approximately 1% in intensity. Although this is a small reduction and could be incorporated into method uncertainty, the issue of a cubic detector in a round pipe could possibly be addressed by: asymmetric lead enclosure, rotational measurement across all axes, or "lighthouse" disc collimation. These three approaches are more fully developed in the following.

Solution 1: Asymmetric Lead Enclosure

Lead greatly reduces the attenuation of radioactive particles. By placing greater amounts of lead on the diagonal of the crystal, it is possible to reduce the influence of particles along this greater displacement.

Solution 2: Rotational measurement across all axes

A more mechanical solution involves the full rotation of the square crystal in order to capture measurements from all angles (Figure 13). This minimizes the effect of varied exposure of a particular location on the pipe wall or location on the crystal.

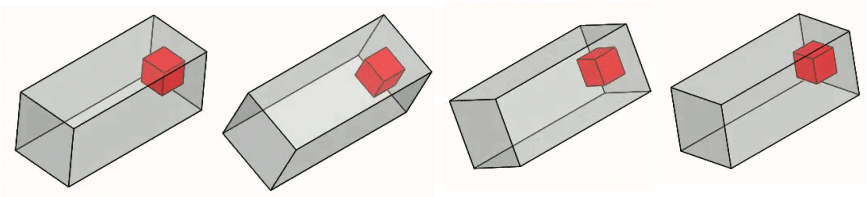

Figure 13: Rotational measurements allow for better elimination of measurement bias.

Solution 3: "Lighthouse" Disc Collimation

A third solution incorporates features of the first two. It creates an asymmetric enclosure to minimize the field of view of the sensor to one face, and then rotates it to measure the full pipe (Figure 14). This reduces uncertainty caused by attenuation through the crystal.

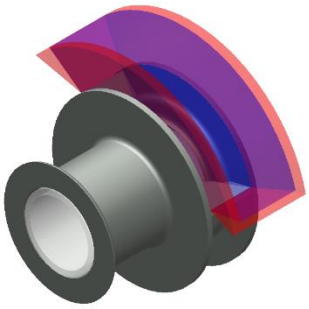

Figure 14: Measurement across a single face eliminates bias caused by non-uniformity of a square crystal.

2.3. Geometry and Imaging Scaling

3D Cameras for Safeguarding

Most commercially available sensors for geometric imaging are designed for room-scale operations. There exist a variety of commercial-off-the-shelf (COTS) sensors for most of the pipe sizes, ranging from 42" down to 6".

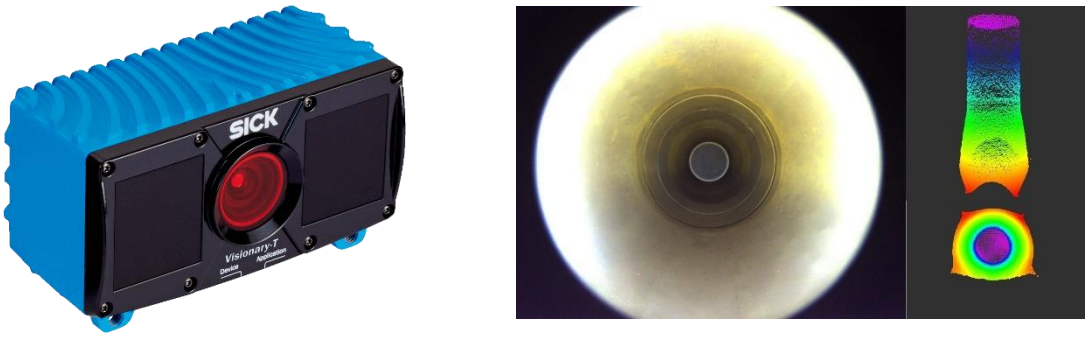

Figure 15: Sick Visionary 3D camera sized 162mm x 97mm x 78mm (left). RadPiper's imagery and 3D point cloud capture (right).

At the pipe sizes designated for RadPiper Jr. (24-36"), the SICK Visionary T provides high-resolution 3D imaging capable of identifying the obstacles present within those pipes. As seen in Figure 15, it is possible to identify pipe geometries such as reducers and wall irregularity. While the Visionary T is a large, industrial-grade sensor, similar technology exists in smaller consumer-grade devices. The Intel Realsense is a similar 3D camera capable of operation in pipe sizes of 8-20 inches.

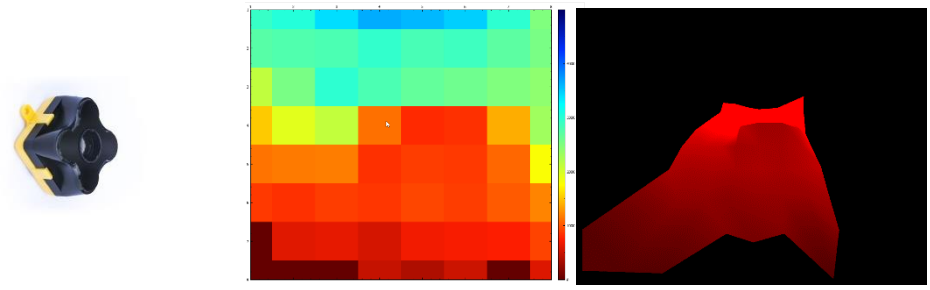

Figure 16: Terabee Evo sized 29mm x 29mm x 22mm (left). Low-resolution point cloud capture of an open end-of-pipe from Evo (right).

As device sizes trend down, performance often follows. Smaller cameras have smaller sensors, which leads to poorer resolution in the captured image. As devices enter the appropriate size for 3" robots, they have fewer than 100 pixels of resolution. One such sensor is the TeraRanger Evo, which is only capable of providing an 8x8 pixel depth map (Figure 16). This leads to a $0.1in^2$/pixel coverage and an inaccurate 3D model of pipe geometry and object detection.

Due to the poor resolution of available sensors, NanoPiper has foregone forward 3D mapping for safeguarding purposes. Based on examinations of floor plans for 3" pipes in typical Uranium enrichment facilities, the only expected obstacles are open and closed pipes. Due to the binary

nature of these obstacles, NanoPiper uses directional point distance sensors in conjunction with image analysis for safeguarding.

Deposit Modelling for Bias Calculations

Geometric measurement of the deposits is also critical for the radiometric method. Due to self-attenuation of Uranium, thicker deposit appears less radioactive than thinner deposit of the same quantity (Figure 17) [8]. This leads to an incorrect estimation of radioactivity when relying on the radiation sensor alone. By measuring the internal deposit thickness, it is possible to account for this bias.

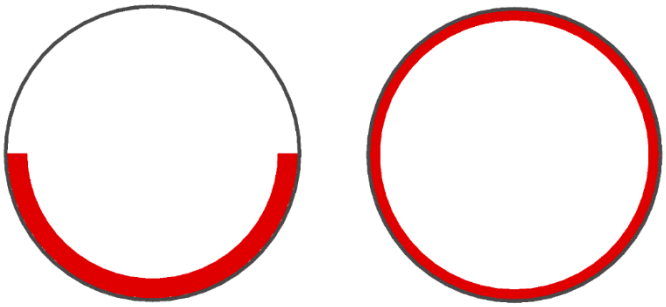

Figure 17: Thicker, non-uniform, deposit appears less radioactive than thinner, uniform, deposit of the same quantity.

The sensing distance for deposits in 3" pipes is often less than 1". At these small distances, LIDARs are a technological impossibility. Another popular technology for this range is a laser triangulation sensor which projects a laser and determines the distance from the geometric displacement of the returned beam [9].

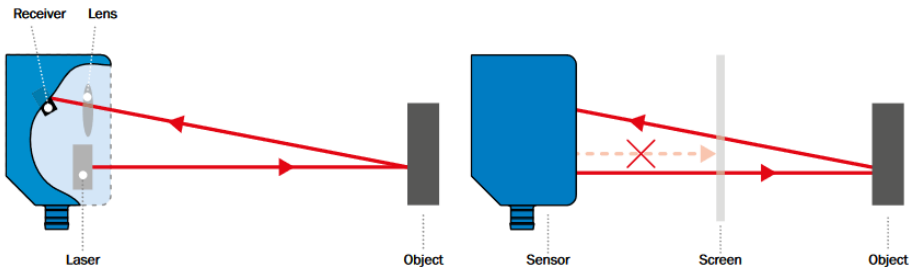

Figure 18: Triangulation sensors measure the geometric displacement by measuring the angle of incidence. [23]

LIDARs are also susceptible to obscuration, as plastic and glass coverings produce inaccurate results [10]. This flaw does not exist with triangulation sensors, as they are fine-tuned for small distance measurements, allowing for the cancellation of short readings (Figure 18) [16].

2.4. Computational Scaling

Primary Computing Module

In-pipe autonomy requires significant computing resources. Robots must collect and log data at up to 100Hz, perform real-time image processing and analysis, and safeguard the robot against all obstacles and pipe conditions.

Computational power often scales proportionally with size; the bigger a PC is, the more power it consumes and the more processing it can do. At large pipe sizes, computing is readily available (Table 3). Quad-core Industrial PCs offer speeds of 2.5GHz and numerous I/O ports for Ethernet, USB, and UART with nominal power consumption of less than 100W.

Table 3: Available computing options for pipe robots.

	Size	Processing	Power	I/O	Memory	Key Feature
R8020 1050Ti	9.5" x 10.3" x 5"	Intel 7th Gen. (3.4 GHz) 1050TI GPU	220W	8x USB 3.0 4x COM 4x PCIe	32GB RAM 1 TB Storage	Dedicated GPU
ML450G11	7.7" x 10.6" x 2.2"	Intel 7th Gen. (2.5 GHz)	60W	6x USB 3.0 4x COM 1x PCIe	8GB RAM 1 TB Storage	General Purpose Computing
CMA24CR	3.8" x 3.6" x 1"	Intel 3rd Gen. (3.1 GHz)	30W	4x USB 3.0 4x COM 10x PCIe	4GB RAM 32 GB Storage	Expandable PCI/104 Interface RTOS
Raspberry Pi 3	3.4" x 2.2" x 0.4"	Cortex A53 (1.2 GHz)	12.5W	4x USB 2.0 40 Pin GPIO	1GB RAM 0 GB Storage	Wide Adoption
Raspberry Pi Zero	2.6" x 1.2" x 0.2"	ARM11 (1 GHz)	0.7W	1x Micro USB 40 Pin GPIO	512MB RAM 0 GB Storage	Ultra-Low Power

Until recently, computing possible in small 3" pipe size was dominated by cheap, poorly supported single board computers. These computers were not documented and had little to no community support. Popular examples include the 'Orange Pi' and the 'UpBoard'. Those widely known, such as the Raspberry Pi, proved too weak to fulfil the requirements. New computers created by NVIDIA fill the void for strong, robust computing with dedicated community resources (Table 4).

These Jetson computers feature a base OEM module and offer numerous 3rd party expansions with different I/O capabilities.

Table 4: Capabilities of NVIDIA Jetson computers.

Name	Size	Processing	Power	I/O	Memory	Key Feature
Xavier	4.1" x 4.1" x 2.6"	ARM v8 512-core Volta GPU	30W	USB CAN / UART SPI / I²C GPIO	16GB RAM 32 GB Storage SATA Expansion	Vision Accelerator
TX2	3.4" x 2.0" Variable Height	Arm v4 256-core Pascal GPU	7.5W	USB CAN / UART SPI / I²C GPIO	8GB RAM 32 GB Storage SATA Expansion	Low Power, High Performance GPU
Nano	2.7" x 1.8" Variable Height	Arm A57 128-core Maxwell GPU	5W	USB CAN / UART SPI / I²C GPIO	4GB RAM 0 GB Storage	Ultra-Small Form Factor

At the time of NanoPiper design, the Jetson Nano was not a commercially available product. As a result, all development is based on the Jetson TX2. The TX2 features numerous carrier boards from a variety of manufacturers.

I/O Module

When comparing PCs, a direct comparison is often difficult to make. Processing power does not correlate directly when factoring into account available system memory and processor generation. However, the trends are evident. As computers get smaller, they consume less power, have less I/O and have more specific computing applications.

Table 5: Available carrier boards for Jetson TX2

Name	Size	I/O	Temperature	Power Req.	Weight
Astro	3.4" x 2.2"	1x USB 3.0, 2x USB 2.0 1x CAN, I²C, Real-time Clock 2x COM (RS-232/485) 1x CSI-2, 3x GMSL	-40°C – 85°C	9V – 36V	46G
Orbitty	3.4" x 2.0"	1x USB 3.0, 1x USB 2.0 4x GPIO I²C, 2x 3.3V UART	-40°C – 85°C	9V – 14V	41G
Aetina AN310	3.4" x 2.8"	2x USB 3.0, 1x Micro USB 2.0 2x CAN, 5x GPIO, I²C 1x COM (RS-232) 6x CSI-2	-40°C – 85°C	9V – 20V	50G
Auvidea J120	4.3" x 2.0"	2x USB 3.0 1x CAN 1x CSI 2x UART, I²C, SPI 1x MPU9250 IMU	-40°C – 85°C	7V – 17V	40G

Numerous I/O boards feature hardware-accelerated image capture, native communication modules, and high-bandwidth USB ports (Table 5). For this application, the J120 proved to be the most useful. Its native CAN and UART enable communication with a vast number of sensors without the need for additional converters. Its high-speed USB 3.0 ports allows the usage of high-resolution cameras and permit the use of multiple cameras in the future.

Recent advancement in computing technology has created a bimodal distribution of processing ability. There exist good solutions at the largest and smallest sizes, but performance degrades for the intermediate sizes, which have varied compute and I/O requirements.

Computational Performance

Ultimately, software performance for PCAMS computing varies moderately between the different processor speeds. The following figures demonstrate the variability in processing power in terms of PCAMS- and ROS-specific requirements [11]:

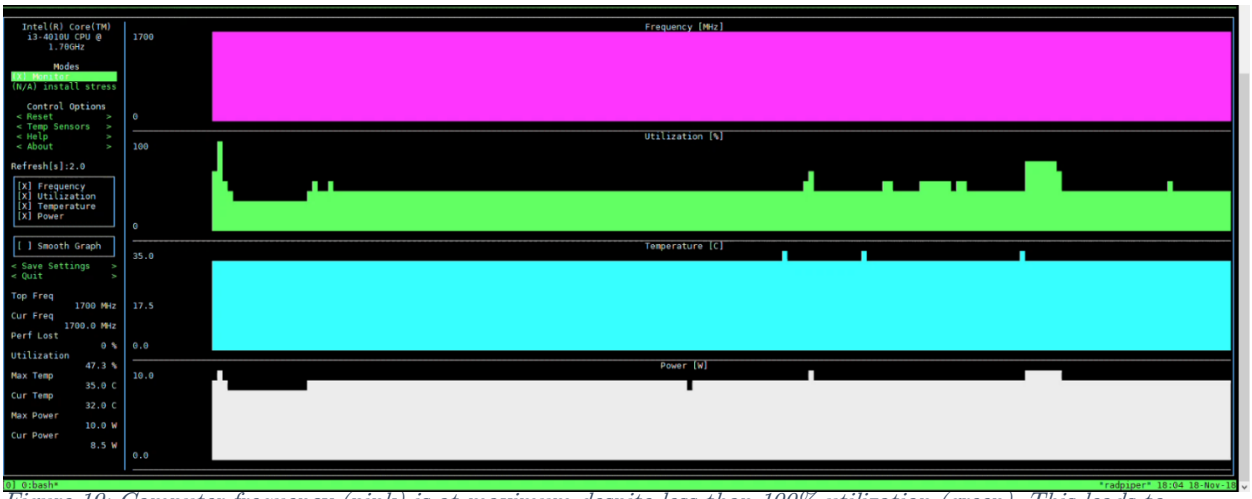

Figure 19: Computer frequency (pink) is at maximum despite less than 100% utilization (green). This leads to increased temperature (blue) and power consumption (gray).

Existing PCAMS scheduling operates the RadPiper computer at its full 1.7GHz processing power. However, utilization is only at 47% (Figure 19), which leads to the conclusion that it is possible to reduce processing speed while still meeting the deadlines imposed by the system. Reduction in speed leads to reduced temperatures and reduced power consumption at the tradeoff of processing time.

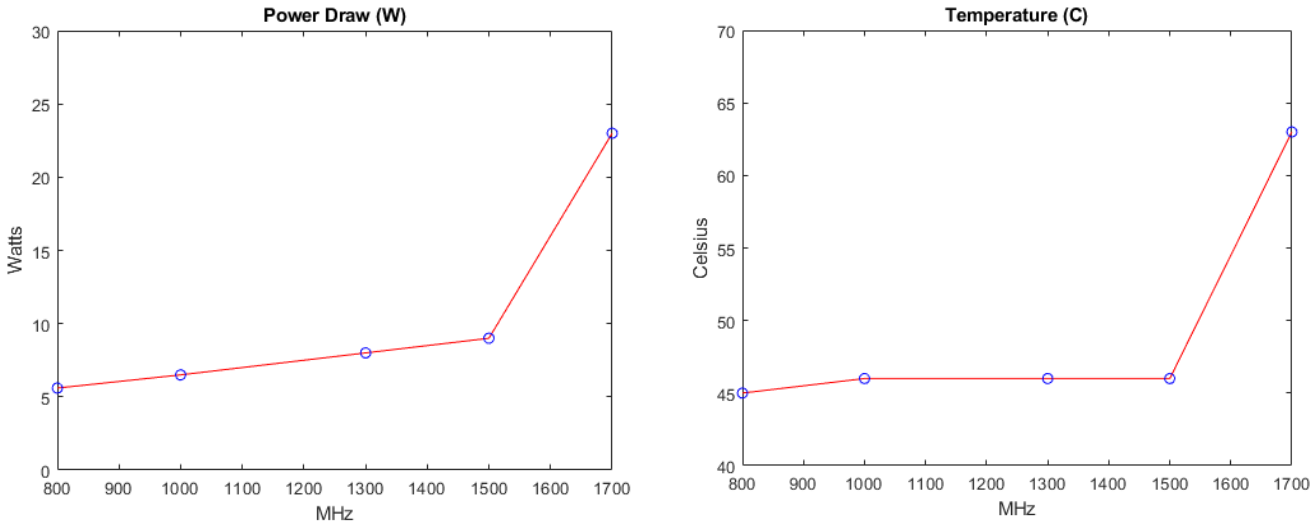

Figure 20: Reduced CPU cluster frequencies lead to drastically reduced power draw and heat generation.

Even though a reduction in processing power leads to reduced temperatures and power consumption, there is a floor (Figure 20). There exist diminishing returns after 1500 MHz in both cases as the power draw and heat generation of the single CPU core are outweighed by the other components on the computer.

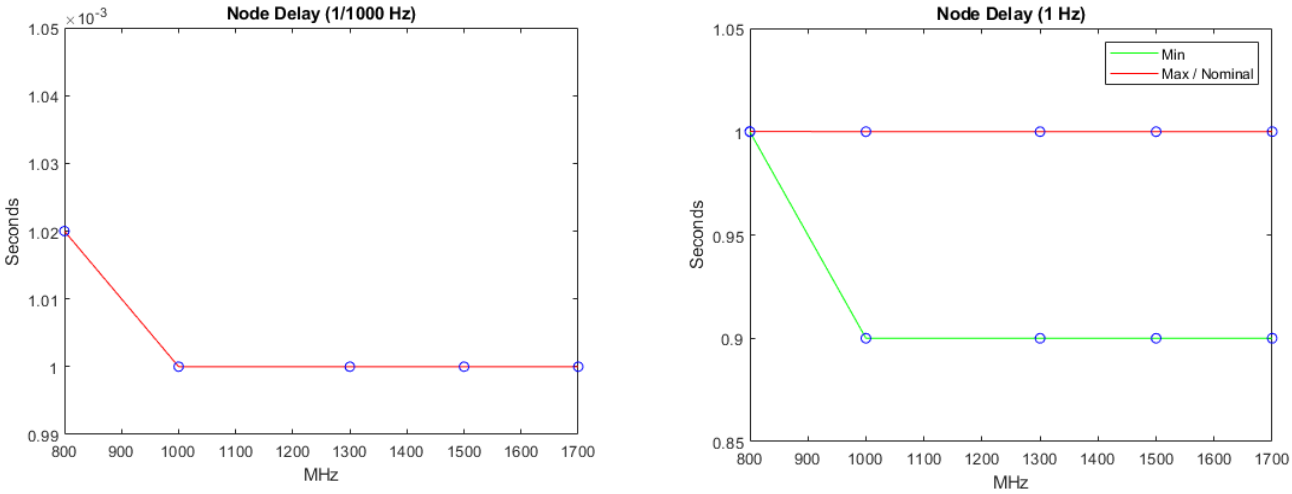

Figure 21: High- and low-frequency node operations are virtually unaffected by reduced CPU speeds.

There are virtually no consequences of reducing the processing speed. In both high-frequency and low-frequency ROS node operation, event rates are virtually unchanged across the CPU frequency spectrum. In the few instances where they are different, nodes are rescheduled earlier than their deadline rather than later. During testing, the CPU was artificially stressed by programs performing arbitrary computations and results may slightly vary depending on the real load of the system.

While nodes themselves have high priority within the ROS infrastructure and have near constant performance, there exists a varied response in message delivery.

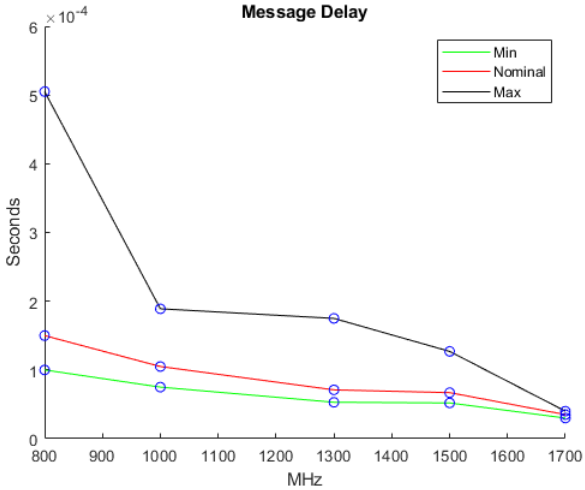

Figure 22: Nominal message delivery times are relatively unaffected by a reduction in processing power; however, delay variance greatly increases.

Reducing processing power from 1700 MHz to 800 MHz increases nominal delivery times by 2x and increases worst-case performance by 5x (Figure 22). Due to the slow travel speed of PCAMS robots, this delay does not create a difficult problem. Nonetheless, PCAMS opts to create three levels of core performance. High-power cores operating at 1700 MHz will run mission-critical tasks, such as safeguarding and autonomy. Medium-power cores operating at 1300 MHz will run mission-essential device drivers such as the radiation sensor and motor driver. Low-power cores operating at 800 MHz will run time-insensitive operations such as data analysis, user interface and post-processing.

Implementing these core affinities leads to an approximately 50% reduction in power consumption by the CPU complex with unnoticeable performance changes during pipe inspection.

2.5. Locomotive Scaling

When determining the appropriate locomotion method for the various PCAMS robots, the tradeoffs between speed, maneuverability, weight, power, material and design difficulty come into consideration.

Generally, wheels require less torque to actuate than treads. This alone makes them the most attractive option in smaller pipes, as smaller motors produce less torque. Existing tread technology is not conducive to miniaturization due to its size, weight and power consumption.

Table 6: Available locomotion options for various pipe sizes.

	Power (W)	Gearing	Pull Rating (Kg)	Operating Temperature (C)	Weight (Kg)	Effective Speed (m/min)	Size (mm)
Minitrac	20	1644:1	22.5	0 - 50°	16.5	1	400 x 80 x 100
Microtrac	72	-	6.5	- 5 - 50°	1.4	9	179 x 56 x 56
Micrometal	1	298:1	0.45	0 - 50°	0.0095	0.6	26 x 10 x 12
Maxon DCX10	1.4	1024:1	1	-30 - 85°	0.0063	0.6	10 x 10 x 18.4

The large size of the tracks precludes its usage in small pipes. The tradeoff for power consumption and mass greatly outweigh the torque requirements necessary for NanoPiper. To that end, NanoPiper uses two micrometal gear motors, each capable of producing 128 mN-m of torque. A single motor can drive the entire system; however, the redundancy allows for gap crossing and deposit traversal.

$$M_{KG} = 5$$
$$C_{RollingResistance} = 0.303$$
$$F_N = M_{KG} * g$$
$$F_{RollingResistance} = F_n * \cos(\theta) * C_{RollingResistance}$$
$$P_{RollingResistance} = F_{RollingResistance} * V_{m/s}$$
$$P_{Lifting} = F_N * \sin(\theta) * V_{m/s}$$
$$P_{Mobility} = \frac{P_{RollingResistance} + P_{Lifting}}{\eta_{\text{motor}}}$$
$$P_{Battery} = \frac{P_{Mobility}}{\eta_{controller}}$$

When operating within piping, NanoPiper primarily needs to overcome frictional force while consuming as little power as possible. Theoretical calculations for the force of rolling resistance, determine that NanoPiper requires 9.26W of electrical power to actuate on a level surface [12]. The force of rolling resistance is negligible at a mere 0.03W of mechanical power, however the inefficiencies within the system are extreme due to the slow travel speeds necessitated by the radiometric method. When attempting to climb inclines of 10 degrees, the lifting power necessitated is 0.02W. When amplified by the inefficiencies, this becomes 16.86W of electrical power. When attempting to climb the maximum slope of 45 degrees, NanoPiper would require 28.17W of electrical power.

Table 7: Drawbar pull test ratings for various tire materials.

	Force Test 1 (N)	Force Test 2 (N)	Force Test 3 (N)	Average (N)
Buna-n	13.32	12.44	12.13	12.34
Polyurethane	11.19	10.93	10.97	11.03
Hard Viton	12.55	13.13	12.25	12.64
Chem-resistant Viton	12.99	13.60	12.58	12.75
EPDM	11.52	10.94	11.42	11.29
Neoprene	11.36	11.44	11.72	11.51
New Silicone	11.53	10.75	10.90	11.06
Used Silicone	11.18	11.73	11.38	11.43
Hi-temp Silicone	11.18	11.38	11.34	11.60

NanoPiper aims to use easily replaceable tires to simplify the robot decontamination process after each run. NanoPiper wheels are a combination of anodized aluminum rims with O-ring tires. These tires make replacements low-cost and readily available. O-rings come in a variety of materials and hardness, making it difficult to identify the proper material at first glance. After testing, it is evident that it does not matter much (Table 7). Most materials are within 1N of traction force. It is of greater importance to prioritize the absorptive properties of the O-ring with regard to radioactive contamination.

Additional consideration needs to be given to the drive controllers. They often do not provide the proper interfaces to be used interchangeably and have tradeoffs in terms of size, communication standard, and interface ports. Industrial controllers are often more robust and have greater I/O at the cost of increased design and integration complexity (Table 8).

Table 8: Available motor controllers for various pipe sizes.

	Interface	I/O	Feedback	Physical Characteristics	Power
RoboClaw	USB / TTL Serial RC Pulse Analog Voltage	5 Input	Inc. Encoder	74 x 52 x 17 mm 60 g	IN: 6 – 34V OUT: PWM @ 15 A Dual Channel
ELMO Gold Twitter	CAN RS232	None	Abs. Encoder Inc. Encoder Digital Hall	35 x 30 x 11.5 mm 18.6 g	IN: 8 – 55V OUT: PWM @ 80A Single Channel
Copley Accelnet Micro	CAN RS232	10 Input 3 Output	Inc. Encoder Digital Hall Resolver	63.5 x 40.6 x 21 mm 37 g	IN: 14 – 55V OUT: PWM @ 6A Single Channel

Ultimately, the dual-channel capabilities of the RoboClaw make it the most appealing choice for smaller robot sizes. Its simple interface allows integration with any computing system without the need for special communication hardware or kernel modules.

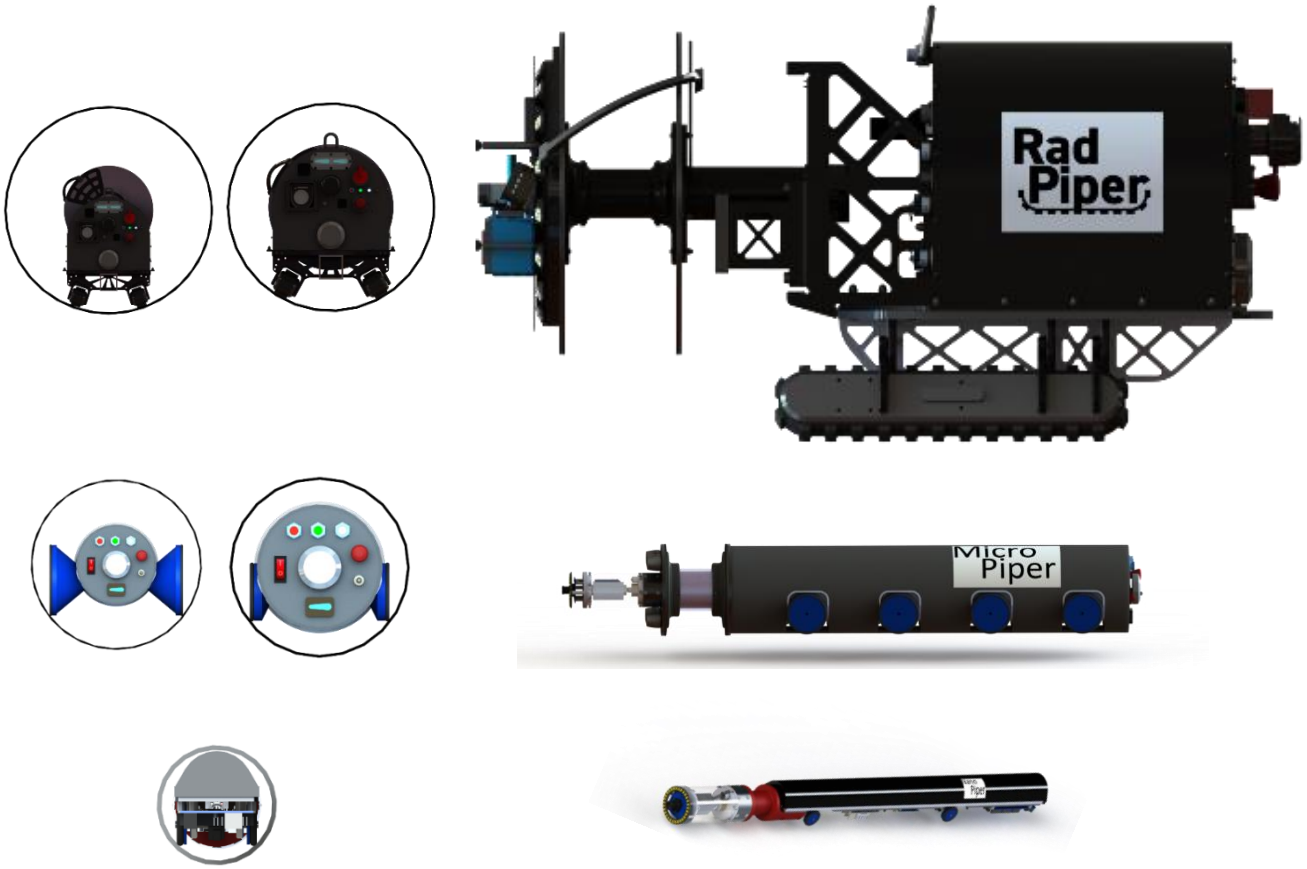

Figure 23: Locomotive options for various pipe sizes. Larger sizes require greater power and obstacle traversal capabilities.

Scalability of locomotion is straightforward: bigger pipes require larger contact areas to maintain centering within the pipe. Larger pipes allow for greater deposit buildup, which increases the requirements for motion. Wheels offer very little weight distribution and cause the robot to sink into the deposit. As a result of increased friction, greater power is required. Additionally, wheels require precision placement to center the radiation sensor. As pipe sizes increase, wheel diameters and distances need to increase. Above 12 inches, treads become the locomotive method of choice due to increased weight and speed requirements. Figure 23 provides concepts for various pipe sizes and robot configurations.

2.6. Localization

Localization technology for large pipes can incorporate large point range LIDARs, full 3D scanners, higher-resolution encoders and can exploit the clear sightline afforded by the large diameters. Miniaturized robots for small pipes are not afforded these luxuries.

Radiometric inspection requires extremely precise and certain localization. It is not just important to know exactly how much Uranium exists, but to know exactly where it exists. Existing methodology for localizing robots does not work well in 3" piping.

Visual Odometry

Proposed visual odometry techniques [13] perform well in the presence of obvious features such as pipe joints and deposit imprints; however, those are few and far between. Most uranium pipes are featureless (Figure 24).

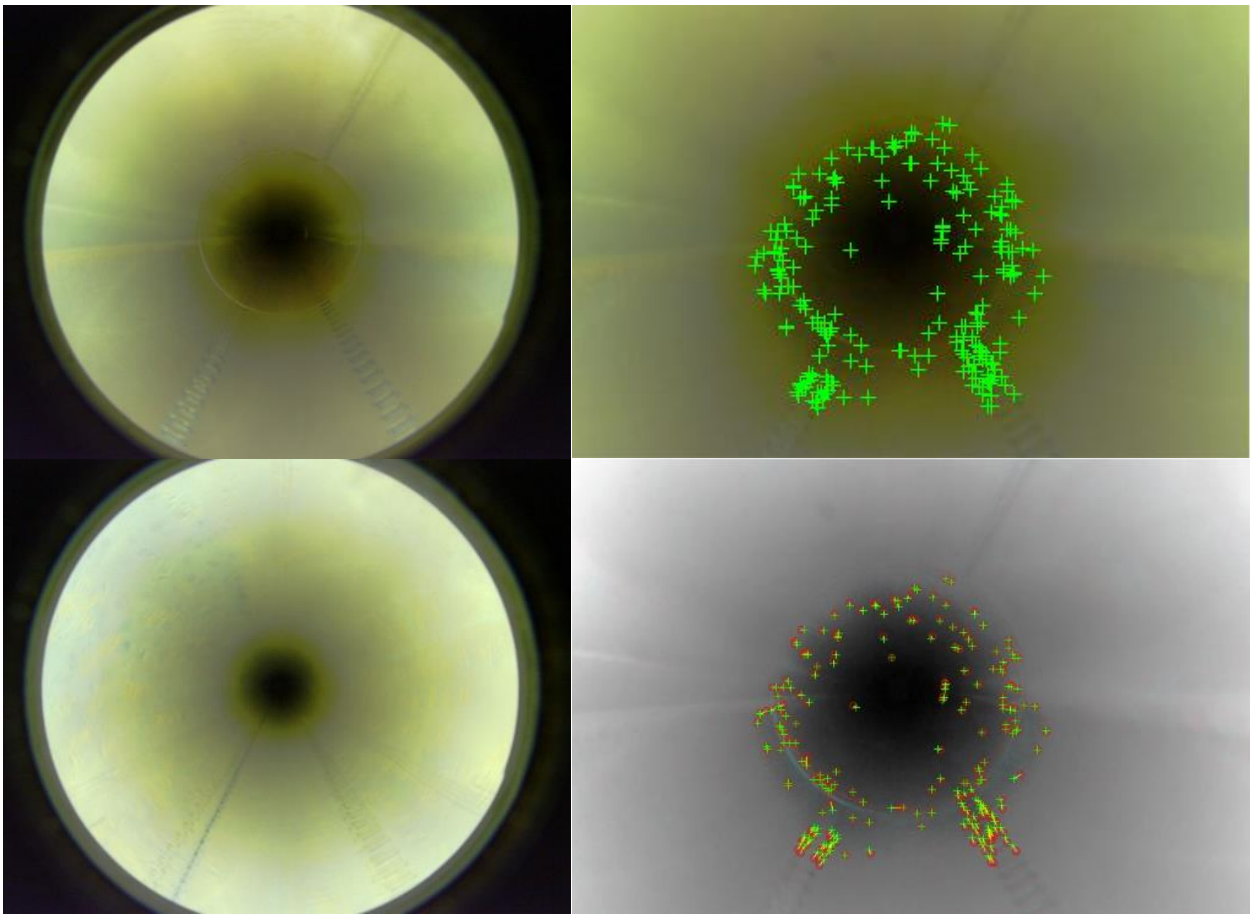

Figure 24: Minimalistic feature set inside 42" piping (top-left). Strongest Harris [14] corner points within image (top-right). Detected translational motion between successive frames (bottom-right). Nominal imagery from inside pipe (bottom-left).

Harris corner points [14], used to identify keypoints, easily recognize small-distance movements between tracks and pipe joints. As pipe sizes decrease, visual features decrease as well. Smaller pipe volumes lead to smaller deposit build-up, which reduces the likelihood of identifiable pipe-wall peeling or deposit formations.

Acoustic Odometry

Additional localization methods involve the use of a laser range finder, such as the one used on RadPiper. These register against a fixed backboard and provide very accurate results if there is an unobstructed view. In a 42" pipe, RadPiper has a maximum measurement distance of 100' due to geometric constraints. Even prior to this maximum distance, a laser range finder produces ambiguous readings due to imprecise pitch and yaw control. This leads to an effective max range of 100'.

Within a 3" pipe at a distance of 20', the laser loses sight of the launch rig with an angular displacement of 0.7 degrees. At the nominal run length of 100 feet, the maximum angular displacement is 0.0025 degrees – a standard impossible to reach.

Instead, NanoPiper implements a one-dimensional localization method using sound waves, known as acoustic odometry. Using the doppler frequency shift, it is possible to determine velocity of the robot at a single point in time. NanoPiper measures an acoustic wave of 210 Hz emitted from the start of the pipe. Traditional localization methods involve time-of-flight calculations, which have maximum ranges of 20m [15]. With nominal runs greater than 30m, such technology is not sufficient.

1: **procedure** ACOUSTIC ODOMETRY
2: $wave \leftarrow audio\ input$
3: $filtered \leftarrow bandpass(wave, emitted\_hz)$
4: **while** $amplitude[i] \neq 0$ **do**
5: $cycle[i] \leftarrow amplitude[i]$
6: $observed\_hz \leftarrow frequency(cycle)$
7: $\Delta f \leftarrow emitted\_hz - observed\_hz$
8: $c \leftarrow speed\ of\ sound$
9: $v(t) \leftarrow \frac{\Delta f * c}{emitted\_hz}$
10: $Distance \leftarrow \int_0^\infty v(t)dt$

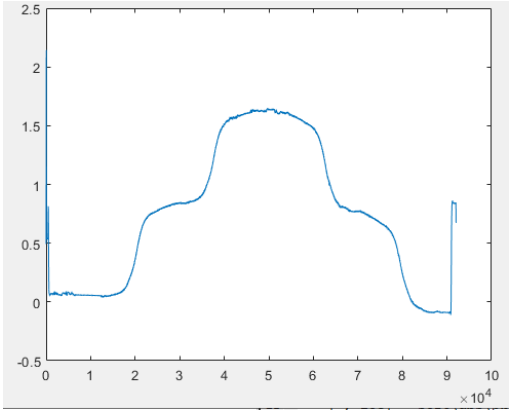

Figure 25: Generalized algorithm for processing acoustic data (left). Generated plateaus that appear ever 2.5 ft for precise localization (right).

By processing this signal, NanoPiper is able to determine the Doppler velocity. Localization via Doppler velocity often does not work well in other environments due to poor transmission in air. Other experiments with 2D Doppler localization have errors up to 10% [16]. However, when inside a pipe, the pipe acts as a waveguide, allowing for a near-perfect transmission of the signal [17].

In the larger pipe sizes, this integration is near continuous. However, when operating within the smaller pipes, processing provides a less continuous waveform. Instead, this algorithm generates plateaus that appear at a fixed distance at 2.5ft. intervals (Figure 25). These plateaus are used as fiducials for absolute localization.

By extending the factor-graph optimization [18] implemented by the PCAMS post-processing system [3], NanoPiper is able to incorporate another landmark (acoustic fiducial) to fuse with those generated by the encoder and visual systems.

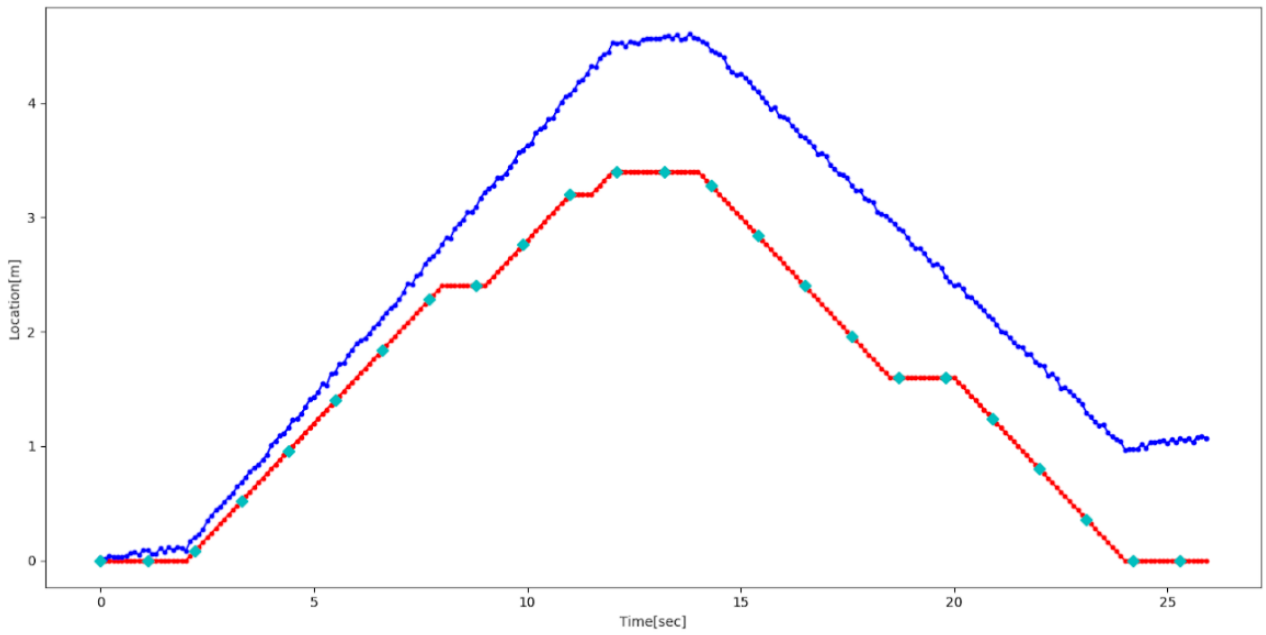

Figure 26: Robot distance as determined by acoustic fiducials (teal) with ground truth (red) and encoded distance (blue).

In 3" pipes, acoustic odometry error is less than 1" in a 60" run (Figure 27). This 2% error is consistent in longer pipe runs, even as far as 240". Acoustic odometry accuracy is independent of pipe size. While pipe diameter and length does affect sound frequency, the noticeable effect is only visible at the exit of the pipe. Nevertheless, end-pipe corrections are possible to account for this phenomenon [19]. Empirical testing has shown viability of this methodology in both 3" and 42" piping making this an acceptable solution for all pipe sizes.

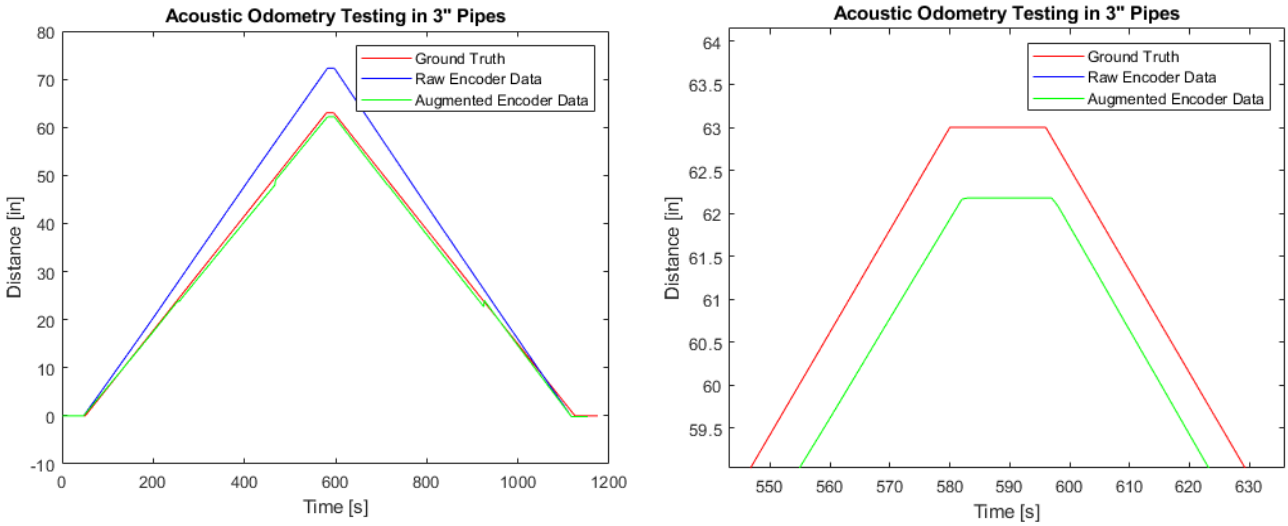

Figure 27: Empirical testing of acoustic odometry. Error is less than 1" in 60" trial runs (<2%).

NanoPiper Hardware

3.1. Modular Connector

Modularity is the core of NanoPiper design. Every module produces a common interface of 20 power pins and 20 signal pins. Due to this common interface, all modules are interchangeable and can be combined to produce different robots using subsets of all available modules.

Each module has a custom-designed PCB that uses pogo pins to establish the connections between the modules (Figure 28). Each spring-loaded connector is of 0.1" pitch, compressible up to 0.04" and can deliver 2A per contact. The modular connector uses two mating pins to help users align the pogo pin with the pogo target. Once aligned, the user compresses and rotates the quick-connect coupler to hold the two modules in place. This design uses Molex FFC ribbon cable to transfer signals within the module, allowing for a passthrough mechanism while using a negligible volume reserved for the robot.

Due to this easy-to-fabricate common interface, it is easy to design multiple independent modules that can be reused for larger size classes.

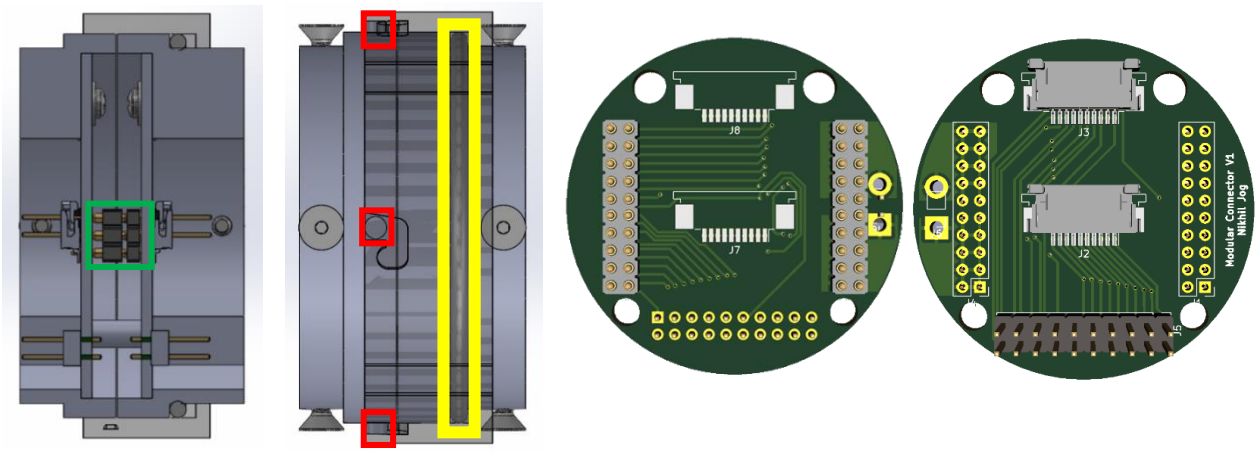

Figure 28: Joint 1 mated with joint 2 (left). The outer ring compresses the O-ring (yellow) to allow rotation onto the locking pins (red). In the locked position, compressible POGO pins (green) provide signal transfer via the custom PCB (right).

3.2. Battery Module

The NanoPiper battery module is a 5.25" long cylinder with a 2.22" diameter (Figure 29). The module houses a Li-ion battery, one set of idler wheels and an optionally insertable rear-USB housing for more I/O.

NanoPiper uses a custom battery composed of four NCR18650PF cells. It has a nominal voltage of 14.4V and 42Wh of power. It features internal circuitry for protection against over-charging, over-discharging, over-drain and short circuiting.

Table 9: Empirical NanoPiper power consumption at various stages of operation.

Component	Standby (W)	Radiometric Quality Control (W)	Inspection (W)
Radiometry	0	0.25	0.25
Mobility	0	0	6
Computing	5	7	20
Profiling	0	0	3.75
Sensing	0	0	1
Total Power	**5**	**7.25**	**21**

During continuous operation, NanoPiper rarely enters the standby phase. A single run consists of 2 quality control checks, a forward run and a reverse run. Experimental testing has shown that NanoPiper is capable of operation for three hours.

Figure 29: Battery compartment, sized 5.25" in length by 2.22" ⌀, houses a 42Wh battery at 14V.

3.3. Radiation Module

The NanoPiper radiation module is a 5"-by-2.2" diameter module which houses a miniature GR1 CZT Spectrometer enclosed in a lead-collimated housing. Recent advances in sensor technology have made NanoPiper possible. The GR1 is a lightweight detector of size 25 x 25 x 63 mm that consumes less than 250 mW of power (Figure 30). The $1cm^3$ CZT crystal provides a greatly improved full-width-half-max (FWHM) resolution compared to the previously used NaI scintillator. This greatly improves identification of the proper isotopes and allows for better quantification of the detected radiation.

Within the housing is an Americium-241 quality control source placed directly against the face of the detector. This check source provides a known amount of radiation that allows the robot to account for background radiation and provide consistently accurate measurements.

The lead collimation disks feature a clamp-mechanism that allows for easy adjustment of the collimation distance. This allows the same module to be used in both 6" and 8" piping, as the FOV can be appropriately set.

Figure 30: Collimated radiation module (left), with small Kromek CZT detector (center), exposing a USB interface (right).

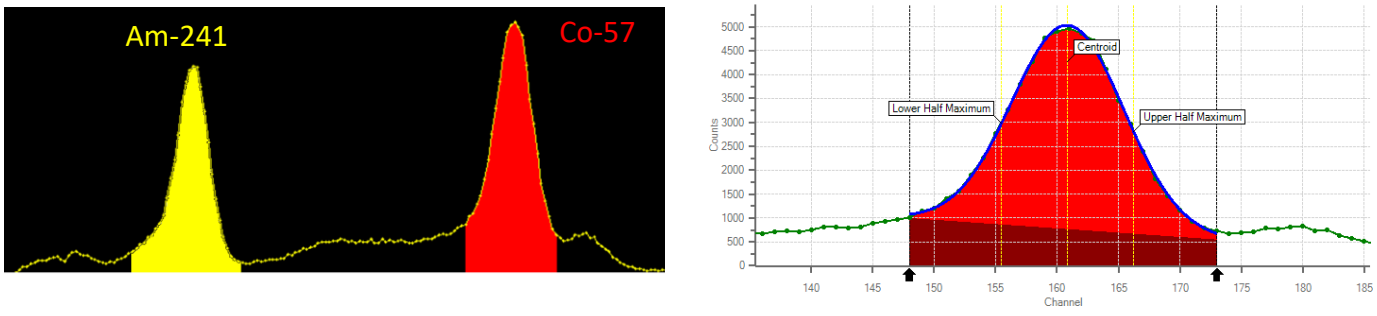

Figure 31: Spectra collected from 10uCi of Co-57 and 1.8435 uCi of Am-241 (left). The ROI for Co-57 produces a full-width-half-max of 10.73keV (right).

Ultimately, a smaller crystal must be capable of producing valid radiometric measurements. Validity is determined by the quality of the peaks generated when measuring the quality-control source (Am-241) and the Uranium analogue (Co-57). Figure 31 demonstrates one such capture, proving. There are two distinct and easily identifiable peaks, proving the viability of a smaller detector in a 3" pipe.

3.4. Compute and Mobility Module

NanoPiper uses a Jetson TX2 with an Auvidea J120 carrier board (Figure 32). The TX2 is an embedded computing device featuring a GPU for efficient machine learning and computer vision processing. Its small form-factor makes it optimal for integration and provides the required processing power for visual safeguarding and feature identification. The TX2 has a variety of I/O boards which provide different ports based on the use case. The J120 carrier board features two USB 3.0 ports, two 3.3V TTL Serial UART ports, two CAN ports, an MPU-9250 IMU and a built-in microcontroller.

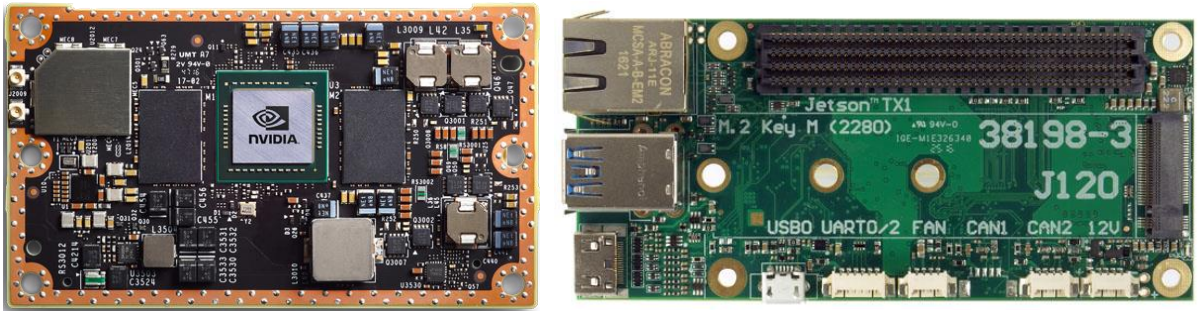

Figure 32: Base TX2 OEM module (left) and J102 carrier board featuring USB 3.0, CAN, UART and Ethernet (right).

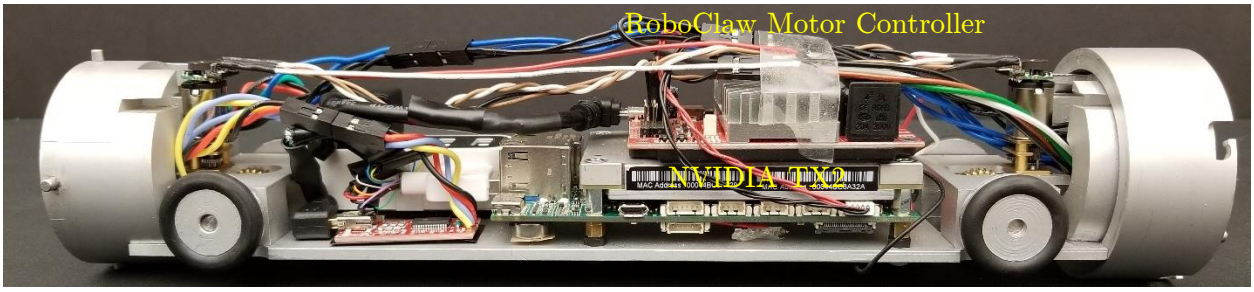

Figure 33: NanoPiper compute and mobility module featuring easily removable tires, RoboClaw motor controller and Jetson TX2.

The TX2 runs the Robot Operating System (ROS) with a custom autonomy pipeline. Robot autonomy monitors the numerous onboard sensors. Due to the distributed nature of the robot, little data processing is done on the TX2. Auxiliary computing sources closer to the sensors analyze the data and produce determinations for the autonomy system.

Figure 34: Micrometal gear motor sized 26mm x 10mm x 12mm (left). Optional hall-effect encoder (right).

This module also contains two micro-metal gearmotors (Figure 34) in a worm gear drive train with a net reduction of 1000:1. Theoretical calculations estimate that NanoPiper requires 128 mN-m of torque to operate. A single motor produces 324 mN-m of torque. NanoPiper's dual drive

redundancy allows for operation over gaps and deposits. This drive assembly is easily removeable, allowing for upgrades in both wheel and motor sizes for larger pipe sizes.

Each motor is also equipped with dual-channel Hall effect sensors that produce 14400 counts per inch of robot travel. Empirical testing has shown that each motor consumes approximately 0.25A in flat pipes and has an encoder error of 0.4 - 4% depending on the length of the run.

Drawbar pull testing of NanoPiper reveals that it produces 10N of force. This indicates that the robot would not be able to move vertically within pipes if equipped with magnetic wheels. Currently, NanoPiper is capable of movement on 25-degree inclines when in motion and 15-degree inclines when starting from a standstill.

Due to the idler wheels on the front and rear, NanoPiper is capable of both gap and deposit traversal under certain conditions. Due to the small clearance in 3" pipes, it is impossible to traverse deposits greater than 0.1", making this essentially not an option. However, in larger pipes greater thicknesses can be traversed. The minimum wheel-wheel distance is 8", making that the largest theoretical gap that it can cross. Empirical testing has shown that NanoPiper is able to cross gaps of up to 5".

3.5. Profiling Module

NanoPiper uses an off-the-shelf SICK OD-Mini inside a custom rotating housing. The OD-Mini comes in various models that offer measurements from 0.4" to 8" all within the same form factor. Each sensor can report up to 500 measurements per second with repeatability of 20μm.

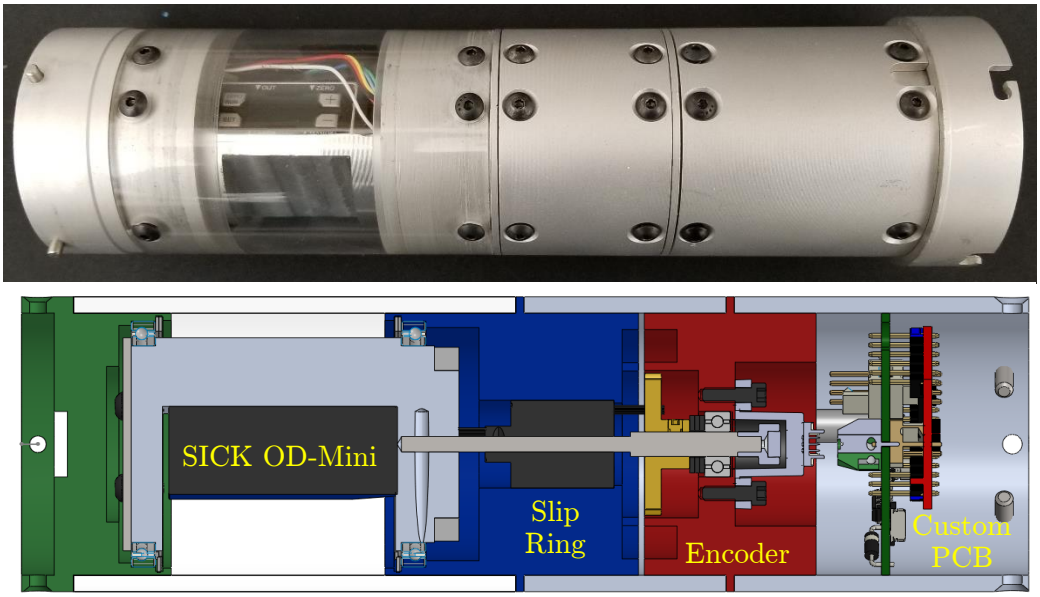

Figure 35: Fabricated profiler (top) along with cross-sectional view (bottom). The profiler is composed of a SICK ODMini, a slip ring, micrometal gearmotor, magnetic encoder and custom data processing PCB.

The housing uses a small, high RPM micrometal gearmotor to rotate the sensor up to 6 revolutions per second (Figure 35). Under nominal operation, the profiler provides sub 2-degree angular resolution across the pipe wall (Figure 36). A custom-designed PCB within the profiler provides low-level matching between rotational encoding and distance measurements so that the primary computer does not need to maintain any inherent timing. The profiler computing is performed by an AST CAN-485 microcontroller which communicates with the OD-Mini via native RS-485 and

the TX2 via TTL Serial. Figure 37 shows a sample point cloud along with a triangulated mesh of the pipe wall [20].

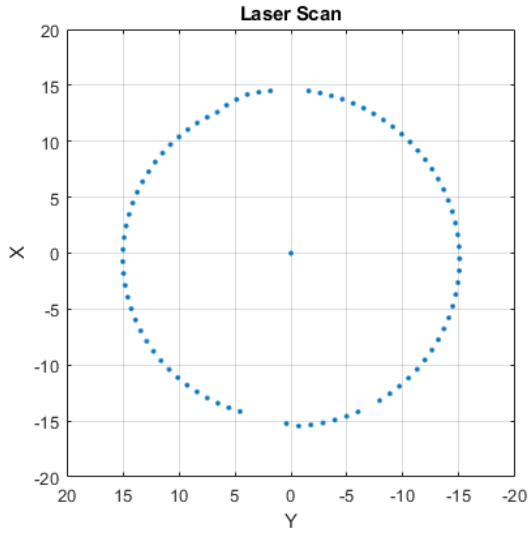

Figure 36: Single laser scan produced by profiler. Reported distance is approximately 15cm with true diameter being 15.24cm. Approximate error is less than 2%.

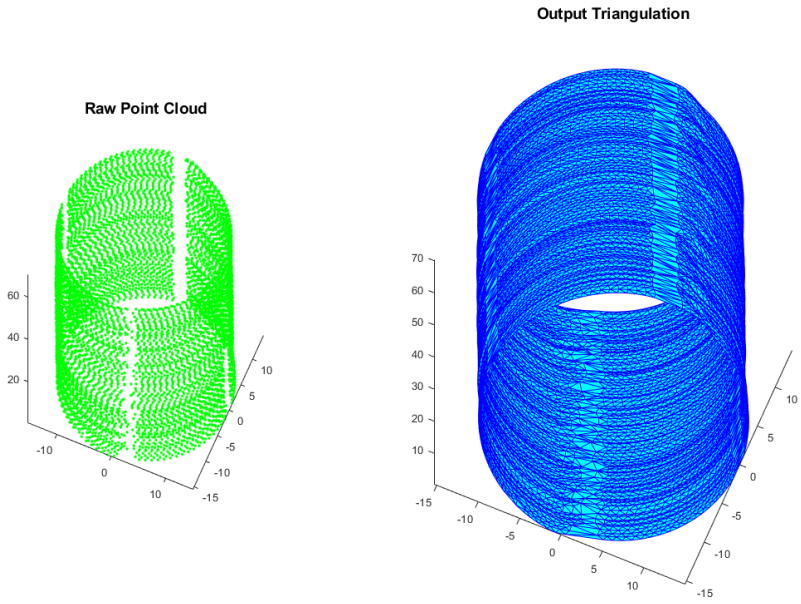

Figure 37: Raw point cloud from 6" piping (left) and triangulated mesh (right). The thick band of empty space is due to a blind spot caused by cables running over the detector.

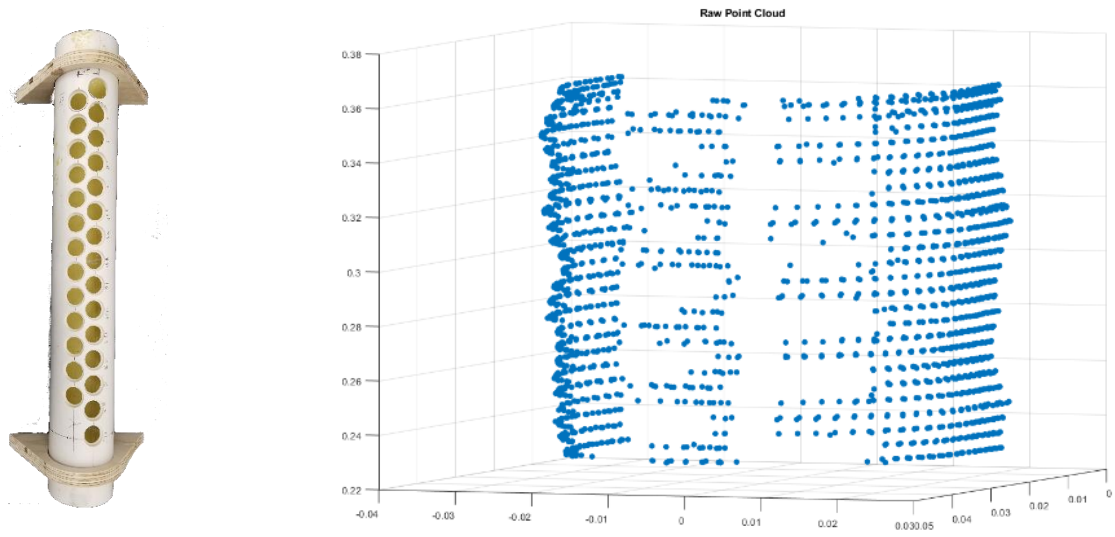

Figure 38: Raw point cloud (right) from 3" piping with drilled holes (left).

This same profiler can also be used for safeguarding. Figure 39 shows a section of a point cloud generated in a 3" pipe. The negative obstacles are clearly visible, allowing for safeguarding via point cloud processing.

Distance measurement sensors exist for all pipe sizes. COTS LIDARs exist for pipe sizes of 10 inches or larger and the custom-designed sensor allows for easy upgrades to the triangulation sensor in all smaller pipes.

3.6. Safeguarding Module

NanoPiper safeguarding is a stand-alone module that provides imagery via a board-mount camera and directional distance via infrared (IR) and time-of-flight sensors.

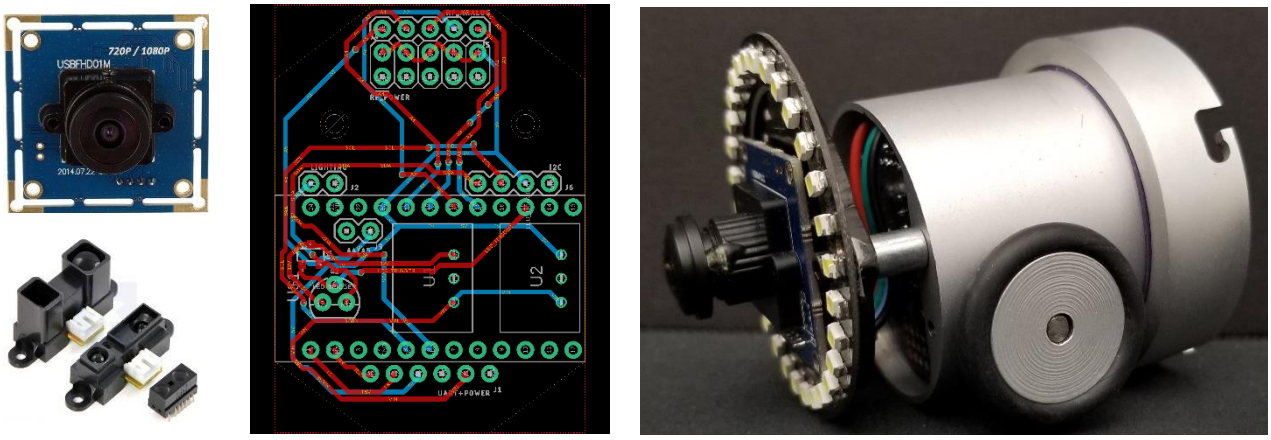

Figure 39: Front safeguarding module (right) featuring IR and ToF sensors, 1920x1080p camera, lighting, and custom data processing PCB.

The safeguarding module uses an AST CAN-485 microcontroller in a custom PCB (Figure 40) to read the analog signals generated from the forward- and downward-facing distance sensor. Based on knowledge of its pipe size, robot clearances and robot length, it determines the ability to continue operation.

```
1: procedure OBSTACLE TRAVERSAL
2:     distance_measured ← read_sensor()
3:     while distance_measured > distance_threshold do
4:         increment_gap()
5:         If gap > gap_threshold then
6:             reverse()
7:         EndIf
8:     while distance_measured < distance_threshold do
9:         for axle in robot_axles
10:            height_variance ← project_robot_forward()
11:            If collides_with_pipe(height_variance) then
12:                reverse()
13:            EndIf
```

Due to the small clearance within 3" pipes, the robot has a limited height of deposit it can traverse. Using the known geometries of the configuration, NanoPiper projects the robot displacement based on the measurements from the downward-facing distance sensor.
Safeguarding scales linearly with the volume of space considered. Larger pipes have greater obstacle avoidance requirements. Detecting those obstacles requires examination of full 3D data rather than the simple 2D analysis perfromed on NanoPiper.

NanoPiper's monocular safeguarding involves numerous stages of object detection and identification. 3" piping within the Portsmouth DOE facility has two primary obstacles: open and closed pipes. Due to this simplification, it is very easy to design a pipeline for these specific instances.

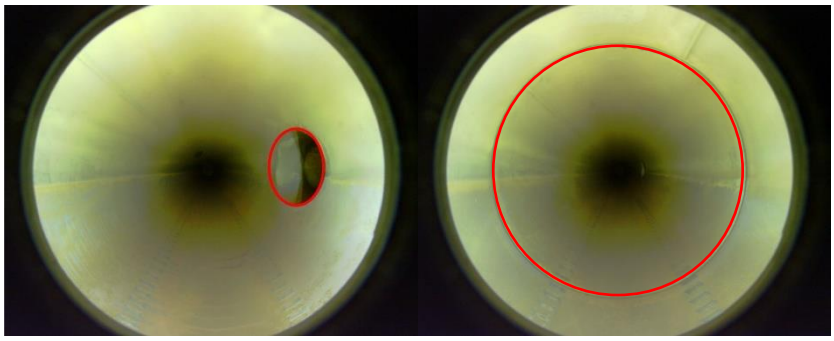

Figure 40: Detected exhaust port (left). Detected pipe joint (right).

The first stage is circle detection using the Hough transform [21] to separate traversable pipe joints from dangerous open/closed pipes. Features such as vacuum ports and swept tees exist in larger pipe sizes, but not in small, 3", piping. Nevertheless, the pipeline identifies and ignores those features.

After detection, analysis of the images in HSV/HSL space helps determine if the terrain after the feature is traversable. The guiding principle behind HSV/HSL analysis is its ability to separate light intensity from color information [22]. Within these pipes, the dominant colors are yellow and black – both of which are difficult to discern in low-light situations. However, when in operation, a reasonable assumption is that the only source of illumination comes from the robot itself. Thus, it is easy to calibrate the expected luma based on experimental testing. Once complete, situations which produce greater amounts of luma are likely a result of light bouncing back at a greater amount, i.e. an obstruction within the pipe. Situations which produce less amounts of luma are likely a result of a lack of pipe wall to reflect the nominal amount of light, e.g., a hole. Figure 41 shows a comparative view of the lighting differences between the two end-of-pipe conditions.

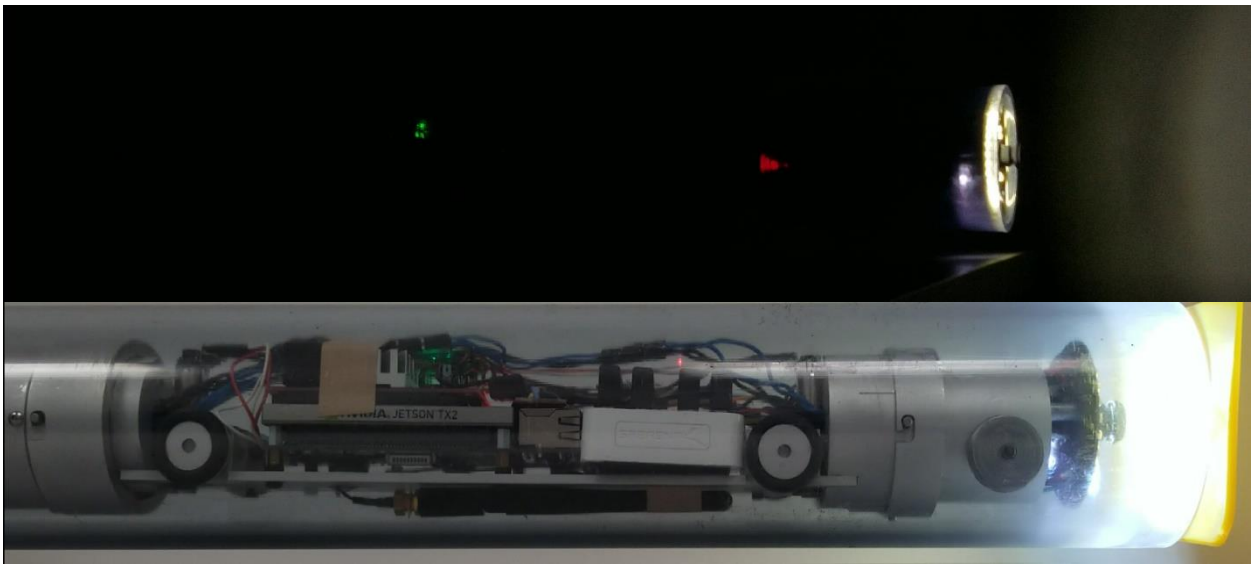

Figure 41: Comparison of lighting differences in open pipes (top) vs. closed pipes (bottom).

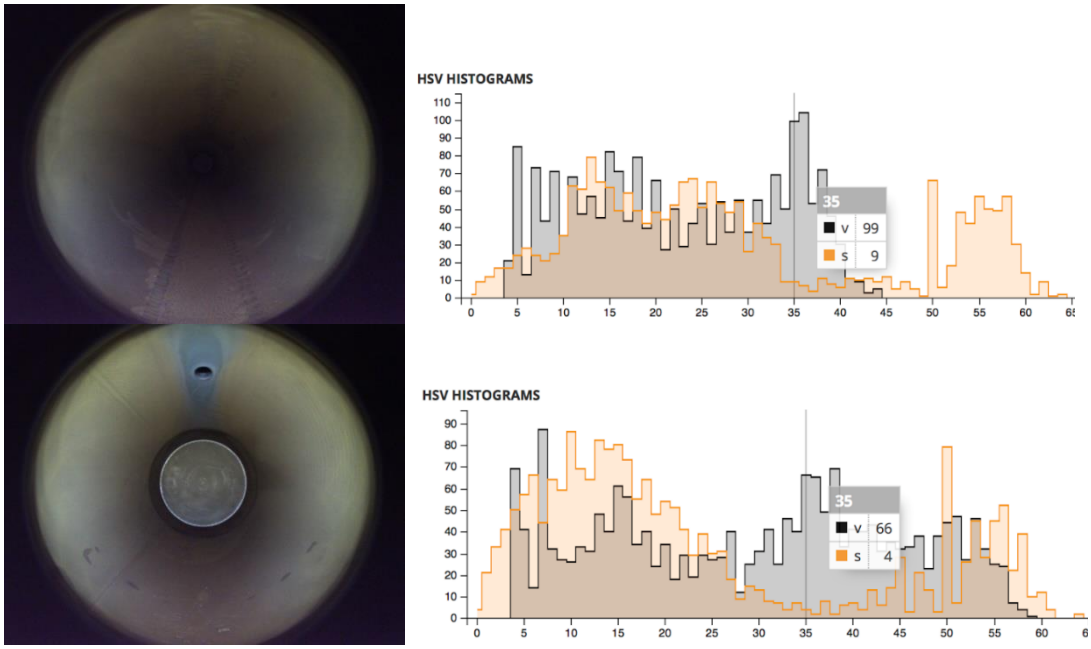

Figure 42: Analysis of captured imagery in HSV/HSL space allows for determination of pipe-end conditions via luma thresholding. Image of an open pipe (top). Image of a closed pipe (bottom).

Figure 42 shows this analysis performed on two scenarios within the pipe. In an open pipe, we see many pixels with high saturation (orange) but few pixels with high intensity (grey). In contrast, in a closed pipe, we see a large increase in both highly- and lowly-saturated pixels. This thresholding is sufficient for end-of-pipe determinations.

Conclusion

4.1. Summary

The research described here addressed and resolved distinctions of miniaturizing in-pipe robotic measurement of Uranium for the smallest pipes in enrichment facilities. To do so, it examined related work, developed methodology, and prototyped a first-of-kind for this robot class. It conceives a configuration for NanoPiper by building modules for power, radiation, locomotion, computing, mapping, and safeguarding that aggregate into a total solution.

Custom-developed sensors not only make small-pipe mapping possible but do so with high accuracy and extensibility. Visual and sensor safeguarding allow the robot to autonomously inspect pipes with and without operator oversight.

Location within a pipe for purposes of Uranium measurement must be more accurate and certain than for any other pipe robot applications. For robots in large pipes, this is achieved with survey-grade laser range sensing and quality odometry not possible on small robots in small pipes. This research developed an innovative and effective means of acoustic odometry that succeeds in small pipes where all other methods fail. Using the principles of Doppler shift, acoustic odometry generates driftless plateaus, which are exploited as periodic fiducials for in-pipe localization.

NanoPiper has proven that in-pipe collection of autonomous radiometric measurements is possible. These systems reduce error, increase repeatability and enable faster and cheaper decommissioning and decontamination.

4.2. Conclusions

Robotic uranium measurement is viable in 3" pipes

NanoPiper is a lightweight, configurable-size robot capable of operating within 3-inch piping. Advances in device technology have directly led to smaller sensors, actuators and computers. Integration of these components have realized autonomous inspection for the smallest of contaminated piping.

Robotic uranium measurement is viable in all pipe sizes from 3 – 42"

The fabrication of NanoPiper in conjunction with prior work on RadPiper not only validates their use in the largest and smallest pipe sizes, but also makes all intermediate sizes a possibility. By changing a few small components, new designs can be built up from NanoPiper or built down from RadPiper. Success in the largest pipe size validates the most difficult radiometric model. Success in the smallest pipe size solves the most difficult mechatronic challenges of this problem.

Reconfigurable robots allow for use of the same robot by consumers with different use cases

The viability of a modular robot is evident in the actualization of an implementation satisfying all functional requirements. Modular components allow for easy upgrades of individual components for larger pipe sizes while retaining the same base. It offers a variety of modules allowing the consumer to choose the specific features for their particular use case.

Acoustic odometry is an innovative and effective means for precise, certain localization in small pipes where all other methods fail

This research developed an innovative and effective means of acoustic odometry that succeeds in small pipes where all other methods fail. We have demonstrated its use in both the smallest and largest of pipes, making it an applicable solution for all sizes in between.

4.3. Future Work

Many improvements are possible. The robot is a prototype requiring rigorous evaluation and refinement and evolution to meet Nuclear Quality Assurance (NQA1) standards.

Further miniaturization, if desired, is possible via custom component development. Motor controllers, for example, are the current size limiter, but could be miniaturized by a customized PCB.

A formal engineering process will greatly improve the stability and integrity of NanoPiper. The development of miniaturized treads for 3" pipes would increase the locomotive power to enable the usage of larger payloads. A custom PCB for acoustic odometry would allow on-board localization with higher fidelity than what is possible today.

NanoPiper exhibits operational autonomy and safeguarding for pipe crawling in critical facilities but is fundamentally a drone that logs data. It is a mechatronic platform to locomote, localize, and collect radiation, geometric and visual data. The great need is to develop post-processing of this data to derive Uranium measurements, correlate those measurements with their corresponding locations, and present findings in user-interface and archival reporting. The model for this is the PCAMS software that exists for NanoPiper's larger RadPiper counterpart.

4.4. Contributions

Creation of NanoPiper is the case proof that the smallest robot for measuring Uranium deposits is achievable in the smallest pipe sizes within nuclear facilities. This required innovations from acoustic odometry to domain-specific configuration and modularity. NanoPiper shows that a family of various robot sizes is feasible for all intermediate pipe sizes from large to small. NanoPiper and its technology are transformational contributions to the nuclear cleanup industry.

NanoPiper is the only autonomous solution for inspection of the smallest of nuclear pipes that demonstrates that all intermediate pipe sizes are possible. NanoPiper is the unambiguous forebear of all future small in-pipe robotic isotope measurement systems yet to come.

References

[1] R. Venkataraman, "Validation of in situ object counting system (ISOCS) mathematical efficiency calibration software," *Nuclear Instruments and Methods in Physics Research A,* vol. 422, 1999.

[2] S. Smith, "Holdup Measurement System 4 (HMS4) - Automation & Improved Accuracy," *Proc. 45th Annual Meeting of the INMM,* 2004.

[3] H. Jones, "Automated Analysis, Reporting, and Archiving for Robotic Nondestructive Assay of Holdup," *WM,* no. 19508, 2019.

[4] H. Jones, "Robotic NDA of Holdup Deposits in Gaseous Diffusion Piping by Gamma Assay of Uranium-235," *WM,* no. 18331, 2018.

[5] Honeybee, "http://www.honeybeerobotics.com/portfolio/pipe-inspection-robot/," [Online].

[6] "http://inuktun.com/en/products/onsite-standard-products/versatrax-50-pipe-inspection-vehicle/," [Online].

[7] T. Kaspar, C. Lavender and M. Dibert, "Evaluation of Uranium-235 Measurement Techniques," 2017.

[8] G. F. Knoll, Radiation detection and measurement, New York: Wiley, 2010.

[9] R. Heitz and S. Mächerlein, "Non-contact measurement with displacement measuring sensors for quality inspection".

[10] M. Schwartz and A. Zarzycki, "The Effect of Building Materials on LIDAR Measurements".

[11] Quigley, Gerkey, Conley, Faust, Foote, Leibs, Berger, Wheeler and Ng, "ROS: an open-source Robot Operating System," 2009.

[12] D. Lippert and J. Spektor, "Rolling Resistance and Industrial Wheels," *Hamilton White Paper,* no. 11.

[13] P. Hansen, H. Alismail, P. Rander and B. Browning, "Monocular visual odometry for robot localization in LNG pipes," *IEEE International Conference on Robotics and Automation,* 2011.

[14] Harris and Stephens, "A combined corner and edge detector," The Plessey Company, United Kingdom, 1988.

[15] D. Marioli, C. Narduzzi, C. Offelli, D. Petri, E. Sardini and A. Taroni, "Digital time-of-flight measurement for ultrasonic sensors," *IEEE Transactions on Instrumentation and Measurement,* vol. 41, no. 1, pp. 93-97, 1992.

[16] Amundson, Koutsoukos and Sallai, "Mobile Sensor Localization and Navigation using RF," ACM, San Francisco, 2008.

[17] Yuan, Liang, Tao, Zou and Cheng, "Broadband directional acoustic waveguide with high efficiency," Appl. Phys. Lett. 101, 20212.

[18] Delaert and Kaess, "Factor Graphs for Robot Perception," *Foundations and Trends in Robotics,* vol. 6, no. 1-2, pp. 1-139, 2017.

[19] M. J. Ruiz, "Boomwhackers and End-Pipe Corrections," 2014.

[20] Gopi, Krishnan and Silva, "Surface Reconstruction based on Lower Dimensional Localized Delaunay Triangulation," 2001.

[21] Ballard, "Generalizing the Hough transform to detect arbitrary shapes," 1980.

[22] D. B. Judd, "Hue Saturation and Lightness of Surface Colors with Chromatic Illumination," *Journal of the Optical Society of America,* vol. 30, no. 1, 1940.

[23] H. Jones, "Results of Robotic Evaluation of Uranium-235 in Gaseous Diffusion Piping Holdup Deposits," *WM,* no. 18303, 2018.

[24] SICK, "Consistent, high product quality thanks to precise optical distance measurement".